Published in final edited form as:
J Biol Chem. 2006 July 28; 281(30): 20958–20973.

Insulin Secretory Responses and Phospholipid Composition of Pancreatic Islets from Mice That Do Not Express Group VIA Phospholipase A_2 and Effects of Metabolic Stress on Glucose Homeostasis*,S

Shunzhong Bao, **Haowei Song**, **Mary Wohltmann**, **Sasanka Ramanadham**, **Wu Jin**, **Alan Bohrer**, and **John Turk**[1]
From the Mass Spectrometry Facility and Division of Endocrinology, Metabolism, and Lipid Research, Washington University School of Medicine, St. Louis, Missouri 63110

Abstract

Studies involving pharmacologic or molecular biologic manipulation of Group VIA phospholipase A_2 (iPLA$_2\beta$) activity in pancreatic islets and insulinoma cells suggest that iPLA$_2\beta$participates in insulin secretion. It has also been suggested that iPLA$_2\beta$is a housekeeping enzyme that regulates cell 2-lysophosphatidylcholine (LPC) levels and arachidonate incorporation into phosphatidylcholine (PC). We have generated iPLA$_2\beta$-null mice by homologous recombination and have reported that they exhibit reduced male fertility and defective motility of spermatozoa. Here we report that pancreatic islets from iPLA$_2\beta$-null mice have impaired insulin secretory responses to D-glucose and forskolin. Electrospray ionization mass spectrometric analyses indicate that the abundance of arachidonate-containing PC species of islets, brain, and other tissues from iPLA$_2\beta$-null mice is virtually identical to that of wild-type mice, and no iPLA$_2\beta$ mRNA was observed in any tissue from iPLA$_2\beta$-null mice at any age. Despite the insulin secretory abnormalities of isolated islets, fasting and fed blood glucose concentrations of iPLA$_2\beta$-null and wild-type mice are essentially identical under normal circumstances, but iPLA$_2\beta$-null mice develop more severe hyperglycemia than wild-type mice after administration of multiple low doses of the β-cell toxin streptozotocin, suggesting an impaired islet secretory reserve. A high fat diet also induces more severe glucose intolerance in iPLA$_2\beta$-null mice than in wild-type mice, but PLA$_2\beta$-null mice have greater responsiveness to exogenous insulin than do wild-type mice fed a high fat diet. These and previous findings thus indicate that iPLA$_2\beta$-null mice exhibit phenotypic abnormalities in pancreatic islets in addition to testes and macrophages.

Phospholipases A_2 (PLA_2)[2] catalyze hydrolysis of the *sn*-2 fatty acid substituent from glycerophospholipid substrates to yield a free fatty acid, *e.g.* arachidonic acid, and a 2-lysophospholipid (1,2) that have intrinsic mediator functions (3,4) and can initiate synthesis of other mediators (5). Arachidonic acid, for example, is converted to prostaglandins,

*This work was supported by United States Public Health Service Grants R37-DK34388, P01-HL57278, P41-RR00954, P60-DK20579, R01-69455, and P30-DK56341.

S The on-line version of this article (available at http://www.jbc.org) contains supplemental figures.

1 To whom correspondence should be addressed: Washington University School of Medicine, Campus Box 8127, 660 S. Euclid Ave., St. Louis, MO 63110. Tel.: 314-362-8190; Fax: 314-362-7641; E-mail: jturk@wustl.edu.

2 The abbreviations used are: PLA_2, phospholipase A_2; BEL, bromoenol lactone suicide substrate; CAD, collisionally activated dissociation; ESI, electrospray ionization; GPC, glycerophosphocholine; HBSS, Hank's balanced salt solution; iPLA$_2\beta$, Group VIA phospholipase A_2; LPC, lysophosphatidylcholine; MS, mass spectrometry; MS/MS, tandem mass spectrometry; PAF, platelet-activating factor; PAPH, phosphatidate phosphohydrolase; PC, phosphatidylcholine; PM, plasma membrane; RT, reverse transcriptase; siRNA, small interfering RNA; SOC, store operated channel; TLC, thin layer chromatography; VOCC, voltage-operated Ca^{2+} channel; WT, wild type; KO, knock-out; au, area units; CT, CTP:phosphocholine cytidylyltransferase.

leukotrienes, and epoxytrienes, and acetylation of 2-lysoplasmanylcholine yields platelet-activating factor (PAF) (5).

Of mammalian PLA_2s so far cloned, the PAF-acetylhydrolase PLA_2 family exhibits substrate specificity for PAF and oxidized phospholipids, and secretory PLA_2 ($sPLA_2$) are low molecular weight enzymes that require mM [Ca^{2+}] for catalysis and affect inflammation and other processes (1). Of Group IV cytosolic PLA_2 ($cPLA_2$) family members (1), $cPLA_2\alpha$ was the first identified and prefers substrates with *sn*-2 arachidonoyl residues, catalyzes arachidonate release for subsequent metabolism, associates with its substrates in membranes when cytosolic [Ca^{2+}], rises, and is also regulated by phosphorylation (6). There are additional members of the $cPLA_2$ family encoded by separate genes (7–10).

The Group VI PLA_2 ($iPLA_2$) enzymes (11–13) do not require Ca^{2+} for catalysis and are inhibited by a bromoenol lactone (BEL) suicide substrate (14) that does not inhibit $sPLA_2$ or $cPLA_2$ at similar concentrations (14–17). The Group VIA PLA_2 ($iPLA_2\beta$) resides in the cytoplasm of resting cells, but Group VIB PLA_2 ($iPLA_2\gamma$) contains a peroxisomal targeting sequence and is membrane-associated(18,19). These enzymes belong to a larger class of serine lipases that are encoded by multiple genes (20,21). The $iPLA_2\beta$ enzymes cloned from various species are 84–88 kDa proteins that contain a G*X*S*X*G lipase consensus sequence and eight stretches of a repetitive motif homologous to that in the protein binding domain of ankyrin (11–13).

It has been proposed that $iPLA_2\beta$ plays housekeeping roles in phospholipid metabolism (22, 23), such as generating lysophospholipid acceptors for incorporating arachidonic acid into phosphatidylcholine (PC) of murine P388D1 macrophage-like cells, based on studies involving reducing $iPLA_2$ activity with BEL or an antisense oligonucleotide that suppresses [^{3}H] arachidonate incorporation into PC and reduces [^{3}H]lysophosphatidylcholine (LPC) levels (23–25). Arachidonate incorporation involves a deacylation/reacylation cycle of phospholipid remodeling (26,27), and the level of LPC is thought to limit the [^{3}H]arachidonic acid incorporation rate into P388D1 cell PC (24,25).

Another housekeeping function for $iPLA_2\beta$ in PC homeostasis has been proposed from studies of overexpression of CTP: phosphocholine cytidylyltransferase (CT) (28,29), which catalyzes the rate-limiting step in PC synthesis. Cells that overexpress CT exhibit increased rates of PC biosynthesis and degradation and little net change in PC levels, suggesting that PC degradation is up-regulated to prevent excess PC accumulation. Increased PC degradation in CT-overexpressing cells is prevented by BEL, and $iPLA_2\beta$ protein and activity increase, suggesting that $iPLA_2\beta$ is up-regulated (28,29).

Many other $iPLA_2\beta$ functions have been proposed (30–43), and the fact that multiple splice variants are differentially expressed among cells and form hetero-oligomers with distinct properties suggest that *$iPLA_2\beta$* gene products might have multiple functions (40–44). Proposed functions include signaling in secretion (40,41,45–50), and BEL attenuates glucose-induced insulin secretion, arachidonate release, and rises in cytosolic [Ca^{2+}] in pancreatic islet β-cells and insulinoma cells (41,45–50).

Many cells, including β-cells, express multiple distinct PLA_2 (13,16,17,51–53), which might reflect redundancy or specific functions of individual PLA_2. The mechanism-based $iPLA_2$ inhibitor BEL and its enantiomers inhibit $iPLA_2$ at concentrations lower than those required to inhibit $sPLA_2$ or $cPLA_2$ (14–17,32), and this has been widely exploited to discern potential biological roles for $iPLA_2$ (30–40,54–56). BEL also inhibits enzymes other than $iPLA_2\beta$; however, including serine proteases (57) and phosphatidate phosphohydrolase-1 (PAPH-1) (58), which accounts for some of its biological effects. In addition, BEL inhibits $iPLA_2\gamma$ (18) and at least four other serine lipases (20,21).

The ambiguity of pharmacologic studies with BEL makes manipulating iPLA$_2\beta$ expression by molecular biologic means an attractive alternative to study iPLA$_2\beta$ functions, and physiological roles for PLA$_2$s can be studied with genetic gain- or loss-of-function manipulations. Stably transfected INS-1 insulinoma cells that overexpress iPLA$_2\beta$ exhibit amplified insulin secretory responses to glucose, particularly in the presence of agents that elevate cAMP (59), and stable suppression of PLA$_2\beta$ expression in transfected insulinoma cells that express small interfering RNA (siRNA) directed against iPLA$_2\beta$ mRNA results in impaired insulin secretory responses to those stimuli (60).

Although these observations support pharmacologic evidence that iPLA$_2\beta$ participates in signaling or effector events involved in insulin secretion (45–51), genetic manipulations at the level of the whole organism sometimes provide information about physiological role(s) of specific gene products that are not readily apparent from results of experiments with cultured cells. Disruption of the gene encoding the Kir6.2 potassium channel, for example, prevents the rise in intracellular [Ca^{2+}] ordinarily induced by D-glucose in pancreatic islet β-cells and suppresses glucose-induced insulin secretion, but, contrary to expectations, non-obese Kir6.2-null mice do not exhibit hyperglycemia because of a counterbalancing increase in insulin action (61), although glucose intolerance can be induced in these mice by dietary interventions and obesity (62,63).

Disruption of the gene encoding cPLA$_2\alpha$ by homologous recombination to yield cPLA$_2\alpha$-null mice has revealed a role for that enzyme in parturition, allergic responses, and post-ischemic brain injury (64,65), and we have generated iPLA$_2\beta$-null mice by similar methods in order to examine the physiological functions of iPLA$_2\beta$ (66). Among various tissues, testes of wild-type mice express the highest iPLA$_2\beta$ levels, and male iPLA$_2\beta^{-/-}$ mice produce spermatozoa with reduced motility and impaired ability to fertilize mouse oocytes. Male iPLA$_2\beta^{-/-}$ mice are much less fertile than wild-type males, but female iPLA$_2\beta^{-/-}$ mouse fertility is not impaired (66).

In this report, we examine the insulin secretory responses and phospholipid composition of pancreatic islets isolated from iPLA$_2\beta$-null mice and their wild-type littermates and the effects on glucose homeostasis of metabolic stresses that include administration of multiple low doses of the β-cell toxin streptozotocin and prolonged feeding of a diet with a high fat content.

EXPERIMENTAL PROCEDURES

Materials

BEL [(*E*)-6-(bromo-methylene)tetrahydro-3-(1-naphthalenyl)-2*H*-pyran-2-one] was obtained from Cayman Chemical (Ann Arbor, MI); enhanced chemiluminescence (ECL) reagents from Amersham Biosciences; standard phospholipids including 1,2-dimyristoyl-*sn*-glycerophosphocholine (14:0/14:0-GPC) and 18:0/22:6-GPC from Avanti Polar Lipids (Birmingham, AL); SDS-PAGE supplies from Bio-Rad; organic solvents from Fisher Scientific; Coomassie reagent from Pierce; streptozotocin, ATP, ampicillin, kanamycin, common reagents, and salts from Sigma; culture media, penicillin, streptomycin, Hanks' balanced salt solution (HBSS), L-glutamine, agarose, molecular mass standards, and RT-PCR reagents from Invitrogen (Carlsbad, CA); fetal bovine serum from Hyclone (Logan UT); Pentex bovine serum albumin (BSA, fatty acid free, fraction V) from ICN Biomedical (Aurora, OH); and forskolin from Calbiochem (La Jolla, CA). Krebs-Ringer bicarbonate buffer (KRB) contained 25 mM HEPES (pH 7.4), 115 mM NaCl, 24 mM $NaHCO_3$, 5 mM KCl, 1 mM $MgCl_2$, and 2.5 mM $CaCl_2$.

Generating iPLA$_2^{-/-}$ Knock-out Mice

The Washington University Animal Studies Committee approved all studies described here and elsewhere in this article. The knock-out construct was prepared with a P1 clone containing an *iPLA$_2\beta$* gene fragment obtained from screening a 129/SvJ mouse genomic DNA library with rat iPLA$_2\beta$ cDNA (66). The 7.8-kb EcoRV-BglII fragment containing exons 7–10 was subcloned into pBluescript SK-(pBSK). A single XhoI site mapped to exon 9. A pGK-neopoly (A) cassette with a neomycin-resistance gene (neo) was inserted at this site to disrupt iPLA$_2\beta$ coding sequence and provide a positive selection marker. This yielded a vector with 4.1 and 3.7 kb of 5′- and 3′-sequence, respectively, homologous to the native gene for recombination.

The targeting fragment was excised with EcoRV and BglII and introduced into 129/SvJ mouse embryonic stem (ES) cells by electroporation. Clones resistant to G418 were isolated and screened for homologous recombination by Southern blotting of genomic DNA digested with EcoRV. Six ES clones contained 6.7-kb fragments characteristic of the disrupted *iPLA$_2\beta$* gene and 8.7-kb fragments from the wild-type allele. Clones were injected into C57BL/6 mouse blastocysts, which were implanted for gestation to yield chimeras that were mated with wild-type mice to yield heterozygotes. Mating iPLA$_2\beta^{+/-}$ mice with each other yielded iPLA$_2\beta^{-/-}$, iPLA$_2\beta^{-/+}$, and iPLA$_2\beta^{+/+}$ pups in a Mendelian 1:2:1 distribution.

Mice were genotyped with Southern blots of tail clipping genomic DNA digested with EcoRV using a ^{32}P-labeled probe (EB) prepared by PCR amplification or by restriction endonuclease digestion with EcoRV and BglII to yield an 0.95-kb fragment located downstream from the targeting sequence. This probe hybridizes with an 8.7-kb DNA fragment in iPLA$_2\beta^{+/+}$ mice, with a 6.7-kb fragment in iPLA$_2\beta^{-/-}$ mice, and with both in iPLA$_2\beta^{+/-}$ mice.

Harvesting Mouse Tissues, Preparing Cytosol, and Extracting Tissue Phospholipids

Mice were euthanized by CO_2 inhalation, and brain, kidney, muscle, aorta, and liver were removed and weighed. Tissue samples (2 grams) were minced and rinsed twice in ice-cold phosphate-buffered saline. To prepare cytosol, three volumes of 67 mM phosphate buffer containing 1.15% KCl were added, and tissue was homogenized in a Dounce apparatus. Homogenates were transferred to centrifuge tubes and centrifuged (10,000 × *g*, 20 min, 5 °C). Supernatants were removed and transferred to Beckman ultracentrifuge tubes and again centrifuged (100,000 × *g*, 1 h, 4 °C). The cytosolic supernatant was removed and stored at −80 °C until use.

For phospholipid extractions, minced tissue (1 g wet weight) was placed in a solution (2 ml) of chloroform/methanol (1:1, v/v) and homogenized (Tissue Tearor, setting 7, 60 s, Biospec Products, Bartlesville, OK). Homogenates were sonicated on ice (20% power, 5 s bursts for 60 s, Vibra Cell probe sonicator, Sonics and Materials, Danbury, CT). Samples were centrifuged (2,800 × *g*, 5 min) to remove tissue debris and supernatants transferred to silanized 10-ml glass tubes and extracted by adding methanol (1 ml), chloroform (1 ml), and water (1.8 ml). Samples were vortex-mixed and centrifuged (900 × *g*, 5 min) and supernatants removed, concentrated, and dissolved in methanol/chloroform (9:1). Lipid phosphorus was measured as described (67).

Islet Isolation

Islets were isolated from pancreata removed from female mice 12–16 weeks of age by collagenase digestion after mincing, followed by Ficoll step density gradient separation, and manual selection under stereomicroscopic visualization to exclude contaminating tissues (68, 69). Mouse islets were counted and aliquoted for insulin secretion studies (30 islets/aliquot)

or analyses of phospholipids (300 islets/aliquot). Islet lipids were extracted, and their phosphorus content was measured, as described above.

Analyses of iPLA$_2\beta$ mRNA in Mouse Tissues

Northern blots of iPLA$_2\beta$ mRNA were performed as described (66). For RT-PCR, total RNA was isolated with an RNeasy kit (Qiagen Inc.). SuperScript First Strand Synthesis System (Invitrogen) was used to synthesize cDNA in 20-μl reactions that contained DNase I-treated total RNA (2 μg). The cDNA product was treated (20 min, 37 °C) with RNase H (2 units, Invitrogen), and heat-inactivated (70 °C for 15 min). A reaction without reverse transcriptase was performed to verify absence of genomic DNA. PCR performed with the pair of primers 1 and 2 was designed to amplify a fragment that spans the neomycin cassette insertion site. PCR performed with the pair of primers 3 and 2 was designed to amplify a fragment downstream from the neomycin cassette insertion site. The sequence of primer 1 is tgtgacgtggacagcactagc; that of primer 2 is ccccagagaaacgactatgga; and that of primer 3 is tatgcgtggtgtgtacttccg.

Western Blotting Analyses and Immunoprecipitation

The proteins in tissue cytosol and membrane fractions were analyzed by SDS-PAGE (7.5%), transferred onto a polyvinylidene difluoride membrane, and probed with iPLA$_2\beta$ antibodies obtained from commercial sources or with antibody 506 provided to us by Dr. Richard Gross, as described in the figure legends. Protein bands were visualized by ECL, as described (13). Immunoprecipitation studies were performed with the Catch and Release® reversible immunoprecipitation system (Upstate Inc., Lake Placid, NY) using iPLA$_2\beta$ antibody obtained from Cayman Chemical (Ann Arbor, MI) according to the manufacturer's instructions.

Identifying a Protein Other than iPLA$_2\beta$ that Cross-reacts with iPLA$_2\beta$ Antibody

Western blotting analyses of cytosol from liver of both wild-type and iPLA$_2\beta$-null mice revealed a 100-kDa immunoreactive band recognized by iPLA$_2\beta$ polyclonal antibody T14 from Santa Cruz Biotechnology. This band was excised from Coomassie-stained SDS-PAGE gels and digested with trypsin, and the digest was analyzed by LC/ESI/MS/MS as described (70). Data base searching revealed a match with mouse glycogen phosphorylase with a high Mascot score of 965. Standard glycogen phosphorylase was then purchased from Sigma, analyzed by SDS-PAGE, and transferred to a nylon membrane. Probing with iPLA$_2\beta$ polyclonal antibody T14 indicated that the 100-kDa protein was recognized by the antibody.

Liquid Chromatographic Mass Spectrometric Analyses of Tryptic Digests of Protein

As described (70), samples (0.2–2 μl) from tryptic digests were injected into a Micromass CapLC liquid chromatography system (Micromass, Manchester, UK). Peptides were concentrated on a PepMap C18 precolumn (300 μm × 5 mm), eluted onto an analytical C18 column (75 μm × 150 mm), and analyzed with a solvent gradient from solution A (3% acetonitrile) to solution B (95% acetonitrile) containing 0.1% formic acid over 50 min at a flow rate reduced from 5 μl/min to 200 nl/min by stream splitting. LC eluant was introduced into the nanoflow source of a Micromass Q-TOF Micro mass spectrometer (Micromass, Manchester, UK). Data-dependent switching from MS to MS/MS analyses was performed, and the resultant data were searched against data bases, as described (70).

Cloning, Expression, and Purification of Polyhistidine-tagged Native iPLA$_2\beta$ and an iPLA$_2\beta$ Mutant Protein Lacking Sequence Encoded by Exon 9

An iPLA$_2\beta$ cDNA that lacked sequence encoded by exon 9 of the iPLA$_2\beta$ gene was constructed using PCR to eliminate exon 9 and to link exons 8 and 10 in a manner that maintained the reading frame. *Spodoptera frugiperda* (Sf9) cells were cultured as described (71). For protein expression, cDNA encoding native iPLA$_2\beta$ with a polyhistidine tag or a cDNA encoding a C-

terminal-polyhistidine-tagged iPLA$_2\beta$ mutant that lacked sequence encoded by exon 9 (NE9-iPLA$_2\beta$) was cloned into the EcoRI-SalI site of pFast-Bac™1 baculovirus shuttle vector (Invitrogen). Sf9 cell suspensions were infected by baculovirus, collected by centrifugation, and disrupted by sonication. His-tagged proteins were purified with a TALON metal affinity column, as described (71). Aliquots of protein solutions were analyzed by SDS-PAGE. Proteins were visualized by Coomassie staining or by immunoblotting after transfer to nylon membranes, as described (13).

Ca^{2+}-independent Phospholipase A_2 Activity Assay

Tissue Ca^{2+}-independent PLA_2 specific activity was determined as described (48) in cytosol by monitoring hydrolysis of 1-palmitoyl-2-[^{14}C]linoleoyl-*sn*-glycero-3-phosphocholine in assay buffer (40 mM Tris, pH 7.5, 5 mM EGTA) to [^{14}C]linoleate as measured by TLC and liquid scintillation spectrometry. Specific activity was calculated from released [^{14}C] dpm and protein content.

Static Insulin Secretion

Islets were rinsed with KRB medium containing 3 mM glucose and 0.1% bovine serum albumin and placed in silanized tubes (12 × 75 mm) in the same buffer, through which 95% air/5% CO_2 was bubbled before the incubation. The tubes were capped and incubated (37 °C, 30 min) in a shaking water bath, as described (68,69). The buffer was then replaced with KRB medium containing 3 or 20 mM glucose and 0.1% BSA without or with forskolin (2.5 or 10 μM), and the samples were incubated for 30 min. Insulin secreted into the medium was measured by radioimmunoassay.

Electrospray Ionization Mass Spectrometric Analyses of Glyc-erophosphocholine Lipids

PC and LPC were analyzed as Li^+ adducts by positive ion ESI/MS on a Finnigan (San Jose, CA) TSQ-7000 triple stage quadrupole mass spectrometer with an ESI source controlled by Finnigan ICIS software. Phospholipids were dissolved in methanol/chloroform (2/1, v/v) containing LiOH (10 pmol/μl), infused (1 μl/min) with a Harvard syringe pump, and analyzed as described (72–74). For tandem MS, precursor ions selected in the first quadrupole were accelerated (32–36 eV collision energy) into a chamber containing argon (2.3–2.5 mtorr) to induce collisionally activated dissociation (CAD), and product ions were analyzed in the final quadrupole. Identities of GPC species were determined from their tandem spectra (72–74), and their quantities were determined relative to the internal standards 14:0/14:0-GPC and 18:0/22:6-GPC by interpolation from a standard curve (60,75,76).

Multiple Low Dose Streptozotocin Administration

Wild-type mice and their iPLA$_2\beta$-null littermates 18–22 weeks of age received 40 mg/kg of streptozotocin (STZ) intraperitoneally on 5 consecutive days between 1300 and 1400 h, as described (77). The mice were housed in a temperature-controlled room with 12-hour light/12-hour dark cycles. Mice were given free access to water and standard laboratory chow during these studies. Blood was obtained at various intervals from the saphenous vein and used for glucose and insulin determinations. Specimens were obtained after an overnight fast. Mice were followed for 7 weeks.

High Fat Dietary Intervention Study

Female mice were housed in a pathogen-free barrier facility with unrestricted access to water and standard mouse chow (Purina Mills Rodent Chow 5053) containing 6% fat. For dietary intervention studies, mice were fed standard chow until 8 weeks of age and thereafter were randomized into groups that were fed either standard chow or a high fat diet continuously for the next six months, as described (78). The composition of the high fat diet (Harlan Teklad

catalog TD88137) was: energy from fat 42%; casein 195 g/kg; sucrose 341 g/kg; corn starch 150 g/kg; cellulose 50 g/kg, anhydrous milk fat (g/kg) 210 g/kg; cholesterol 1.5 g/kg; 18.95 kilojoules per gram.

Glucose and Insulin Tolerance Tests

Female mice in clean cages with free access to water were fasted overnight and then weighed, and baseline blood glucose was determined using Ascensia ELITE XL blood glucose meter. The animals were injected intraperitoneally with 50% (w/v) dextrose at a dose of 2 mg/g body weight, and blood glucose was measured at 30, 60, and 120 min, as described (69). Insulin tolerance tests were conducted in a similar manner, except that mice were not fasted and received an intraperitoneal injection of human regular insulin (Lilly, Indianapolis, IN) at a dose of 0.75 units/kg body weight, as described (69).

Other Analytical Procedures

As described (69), serum glucose was measured using reagents from Sigma. Serum insulin was assessed by enzyme-linked immunosorbent assay (Crystal Chem. Inc., Downer's Grove, IL).

Statistical Methods

Results are presented as mean ± S.E. Data were evaluated by unpaired, two-tailed Student's *t* test or by analysis of variance with appropriate post-hoc tests. Significance levels are described in individual figure legends.

RESULTS

Production of iPLA$_2$β-Null Mice and Characterization of iPLA$_2$β mRNA Expression in Mouse Pancreatic Islets, Brain, and Other Tissues

We recently generated iPLA$_2\beta$-null mice via homologous recombination and observed that they exhibit a phenotype of greatly reduced male fertility associated with impaired production and motility of spermatozoa (66). Expression of iPLA$_2\beta$ was found to be highest in wild-type mouse testes among tissues examined, which did not include pancreatic islets in our first report on iPLA$_2\beta$-null mice, and no iPLA$_2\beta$ mRNA or protein was observed in testes or in other examined tissues from iPLA$_2\beta$-null mice (66).

High levels of iPLA$_2\beta$ are expressed in brain (79), and brain shares many biochemical similarities with pancreatic islets that other tissues do not (80). Another group of investigators (36) informed us that they observed iPLA$_2\beta$-immunoreactive protein in brains of iPLA$_2\beta$-null mice obtained from our laboratory, and this caused us to re-examine iPLA$_2\beta$ expression in brain of iPLA$_2\beta$-null mice to determine whether functional protein might be produced from an alternatively spliced mRNA species derived from the disrupted *iPLA$_2\beta$* gene.

The knock-out construct for disrupting the *iPLA$_2\beta$* gene resulted in insertion of a neomycin-resistance cassette into exon 9, which precedes the GTSTG serine lipase consensus motif encoded in exon 10. This was predicted to alter the reading frame and result in premature stop codons that would cause termination of translation at a point preceding the GTSTG motif. Because we observed no iPLA$_2\beta$ mRNA of any size by Northern blotting or by RT-PCR in iPLA$_2\beta$-null mouse tissues with various primer sets that should have recognized even truncated mRNA species, we concluded that any mRNA produced from the disrupted *iPLA$_2\beta$* gene was rapidly degraded by non-sense-mediated decay.

Nonetheless, several isoforms of iPLA$_2\beta$ arise from alternatively spliced mRNA species in various cells (42–44), and we considered the possibility that an exon-skipping mechanism of

splicing that resulted in exclusion of exon 9 might yield a functional protein that contained the lipase consensus sequence and that such splicing might be tissue- or age-dependent. We therefore performed Northern blotting analyses for iPLA$_2\beta$ mRNA in several tissues including brains from mice aged one month to two years using a probe that recognizes sequence spanning exons 7 through 12 of the *iPLA$_2\beta$* gene. Brain and other tissues, including pancreatic islets, from wild-type mice did contain mRNA species of the expected size that were recognized by the iPLA$_2\beta$ probe, but none of any size was observed in tissues from iPLA$_2\beta$-null mice (Fig. 1*A*).

RT-PCR experiments were also performed with two sets of primers, the first of which amplified sequence in iPLA$_2\beta$ mRNA beginning in exon 6 and extending into exon 14, which spans the insertion site for the neomycin resistance cassette. The second pair of primers amplifies sequence that starts in exon 11 at a point after the neomycin resistance cassette insertion site and ends in exon 14. Each primer set yielded a product of the expected size in wild-type brain, pancreatic islets (Fig. 1*B*), and other tissues, but no such products or any shorter ones were observed in tissues of iPLA$_2\beta$-null mice. These Northern blotting and RT-PCR studies thus indicated that brain, pancreatic islets, and other tissues from iPLA$_2\beta$-null mice contained no full-length or alternatively spliced iPLA$_2\beta$ mRNA species that lacked exon 9.

Expression of iPLA$_2$β-Immunoreactive Protein in Mouse Brain

Because we could demonstrate no iPLA$_2\beta$ mRNA species in tissues of iPLA$_2\beta$-null mice of any age, we suspected that iPLA$_2\beta$ immunoreactive protein observed in brain of iPLA$_2\beta$-null mice was not produced from an alternatively spliced iPLA$_2\beta$ mRNA but rather reflected a non-iPLA$_2\beta$ protein that cross-reacted with iPLA$_2\beta$ antibodies. To examine this issue further, we performed immunoprecipitation studies using an iPLA$_2\beta$ antibody obtained from Cayman Chemical, analyzed the immunoprecipitates by SDS-PAGE, and then performed Western blotting with a second iPLA$_2\beta$ antibody obtained from Santa Cruz Biotechnology.

Fig. 2*A* illustrates such analyses of cytosol from stably transfected INS-1 insulinoma cells (59) that overexpress iPLA$_2\beta$ (lane 1); a parental INS-1 cell line that expresses lower levels of iPLA$_2\beta$ (lane 2); wild-type (lane 3) or iPLA$_2\beta$-null (lane 4) mouse brain; and washes of immunoprecipitates from INS-1 cells (lane 5), wild-type mouse brain (lane 6), and iPLA$_2\beta$-null mouse brain (lane 7). Cytosolic immunoprecipitate from the iPLA$_2\beta$-overexpressing (lane 1) or parental (lane 2) INS-1 cell lines and the immunoprecipitate from wild-type mouse brain (lane 3) all contain an 84 kDa iPLA$_2\beta$-immunoreactive protein that corresponds to iPLA$_2\beta$, but the immunoprecipitate from iPLA$_2\beta$-null mouse brain does not (lane 4). This material is also absent from washes of the immunoprecipitates from INS-1 cells or wild-type or iPLA$_2\beta$-null mouse brain (lanes 5–7), indicating that the immunoprecipitating antibody effectively removed iPLA$_2\beta$ from solution. A number of other proteins are observed in lanes 2–7 that we believe represent cross-reacting proteins that do not arise from iPLA$_2\beta$ mRNA.

Similar experiments were performed with another iPLA$_2\beta$ antibody given to us by Dr. Richard Gross that was prepared in his laboratory (Fig. 2*B*). This antibody recognizes a protein with a molecular mass of 84 kDa in the cytosol of INS-1 cells that overexpress iPLA$_2\beta$ and from brain of wild-type mice, but no such protein is observed in cytosol from brain of iPLA$_2\beta$-null mice (Fig. 2*B*).

We conclude that iPLA$_2\beta$ protein is expressed in brain of wild-type but not iPLA$_2\beta$-null mice and that iPLA$_2\beta$ antibodies recognize a number of proteins other than iPLA$_2\beta$. In support of this, we have identified one of the proteins that cross-reacts with iPLA$_2\beta$ antibodies in liver (see figure in supplemental data) by digesting the cross-reactive band with trypsin followed by LC/MS/MS analyses and data base searching, which identified mouse glycogen

phosphorylase. Authentic glycogen phosphorylase was then purchased and analyzed by SDS-PAGE and Western blotting and shown to cross-react with iPLA$_2\beta$ antibody.

An iPLA$_2$β Mutant Protein That Lacks Sequence Encoded by Exon 9 Is Catalytically Inactive

Although our findings indicated that no iPLA$_2\beta$ mRNA or protein is expressed in iPLA$_2\beta$-null mouse tissues, we wondered whether a catalytically active protein could be produced from an alternatively spliced iPLA$_2\beta$ mRNA species that lacked sequence encoded by exon 9. We therefore prepared a cDNA construct encoding such a mutant protein (NE9-iPLA$_2\beta$) with a polyhistidine tag (Fig. 3*A*), expressed it in a baculovirus-Sf9 cell system, purified it by immobilized metal affinity chromatography, and compared its catalytic activity to that of native iPLA$_2\beta$ with a polyhistidine tag.

Fig. 3*B* illustrates that native iPLA$_2\beta$ catalyzes hydrolysis of the phospholipid substrate 1-palmitoyl-2-[^{14}C]linoleoyl-*sn*-glycero-3-phosphocholine in the absence of Ca^{2+} and that this activity is stimulated by ATP and inhibited by the iPLA$_2\beta$ suicide substrate BEL. In contrast, the mutant protein exhibits no ATP-stimulated or BEL-inhibited PLA$_2$ activity. We conclude that any protein produced from an iPLA$_2\beta$ mRNA species that lacked sequence encoded by exon 9 would not be catalytically active.

Insulin Secretory Properties of Pancreatic Islets Isolated from Wild-type and iPLA$_2$β-Null Mice

Our reports that the iPLA$_2\beta$ suicide substrate BEL inhibits glucose-induced insulin secretion from rat (47) and human (81) pancreatic islets and insulinoma cells (48,49) suggest that iPLA$_2\beta$ might participate in insulin secretion. This is supported by findings that stably transfected INS-1 insulinoma cell lines that overexpress iPLA$_2\beta$ exhibit more robust insulin secretory responses to glucose and forskolin than do parental INS-1 cells (59) and that stably transfected INS-1 cells that produce siRNA that suppresses iPLA$_2\beta$ expression have impaired insulin secretory responses (60). This suggests that iPLA$_2\beta$-null mouse pancreatic islets might exhibit impaired insulin secretory responses, although some mouse tissues express much less iPLA$_2\beta$ than do the corresponding rat or human tissues (82). Fig. 1, *A* and *B* provide the first evidence that mouse pancreatic islets, like those from rats and humans (13,43), do express iPLA$_2\beta$.

Fig. 4 illustrates that insulin secretion from pancreatic islets isolated from wild-type mice is stimulated by 20 mM D-glucose and that this response is amplified by the adenylyl cyclase activator forskolin (2.5 μM), as is also the case for rat and human islets. Insulin secretion from islets isolated from iPLA$_2\beta$-null mice is also stimulated by 20 mM D-glucose and amplified by 2.5 μM forskolin, but these responses are significantly reduced with iPLA$_2\beta$-null compared with wild-type islets. This suggests that the absence of iPLA$_2\beta$ in islets results in attenuation of insulin secretory responses to some stimuli.

Nonetheless, neither the fasting nor fed blood glucose concentrations differed between wild-type and iPLA$_2\beta$-null mice at any age examined, suggesting that *in vivo* compensation occurred for the insulin secretory impairment of isolated islets from iPLA$_2\beta$-null mice. The insulin secretory impairment of iPLA$_2\beta$-null islets at 2.5 μM forskolin could be overcome at 10 μM forskolin, suggesting that the secretory defect of iPLA$_2\beta$-null mice can be overridden under some conditions, and this could explain the apparent normality of glucose homeostasis of iPLA$_2\beta$-null mice under non-stressed conditions.

Phospholipid Composition of Pancreatic Islets and Brain of Wild-type and iPLA$_2$β-Null Mice

It has been suggested that iPLA$_2\beta$ plays housekeeping functions in maintaining PC homeostasis by providing 2-lysophosphatidylcholine acceptors for arachidonic acid incorporation into PC

and by cooperating with cytidylylphosphocholine transferase to maintain appropriate cellular PC levels (22,23,28,29). This suggests that the PC composition of tissues from iPLA$_2\beta$-null mice, particularly the abundance of arachidonate-containing PC species, might differ from that of wild-type mice.

We therefore examined the composition of glycerophosphocholine (GPC) lipids from brain and pancreatic islets of wild-type and iPLA$_2\beta$-null mice as Li^+ adducts by ESI/MS (Fig. 5) and by ESI/MS/MS (Fig. 6). Ions representing arachidonate (20: 4)-containing GPC lipids are prominent in the spectra in Fig. 5 and include those at *m*/*z* 788 (16:0/20:4-GPC) and *m*/*z* 816 (18:0/20:4-GPC). The identities of the parent $[M + Li]^+$ ions were established from their tandem spectra (Fig. 6).

CAD of *m*/*z* 788 yields a spectrum (Fig. 6*A*) that contains ions reflecting neutral losses of trimethylamine plus either the *sn*-1 substituent (MLi^+-315) or the *sn*-2 substituent (MLi^+-363) as free fatty acids at *m*/*z* 473 and *m*/*z* 425, respectively. The former is more abundant than the latter, indicating that palmitate and arachidonate are the *sn*-1 and *sn*-2 substituents, respectively (72–74). Analogous ions in Fig. 6*B* (*m*/*z* 473 and 453) from CAD of *m*/*z* 816 indicate that stearate and arachidonate are the *sn*-1 and *sn*-2 substituents, respectively, of the parent $[M + Li]^+$ ion.

Fig. 6*A* also shows neutral losses of the *sn*-1 substituent as a free fatty acid (MLi^+-256) or as a Li^+ salt (MLi^+-262) at *m*/*z* 532 and *m*/*z* 526, respectively. Ions of the same *m*/*z* values are observed in Fig. 6*B* and represent [MLi^+-284] and [MLi^+-290], respectively. Neutral losses of the *sn*-2 substituent as a free fatty acid (MLi^+-304) or as a Li^+salt (MLi^+-310) are seen at *m*/*z* 484 and *m*/*z* 478, respectively, in Fig. 6*A* and at *m*/*z* 512 and *m*/*z* 506, respectively, in Fig. 6*B*. The ion *m*/*z* 313 (MLi^+-475) in Fig. 6*A* reflects net elimination of $[LiPO_4(CH_2)_2N(CH_3)_3]$ and loss of the *sn*-2 substituent as a ketene (72–74). An analogous *m*/*z* 341 ion (MLi^+-475) is seen in the tandem spectrum 18:0/20:4-GPC-Li^+ (Fig. 6*B*). Other diagnostic ions in Fig. 6*A* include those for loss of trimethylamine (*m*/*z* 729) or net loss of phosphocholine or its Li^+ salt from $[M + Li]^+$ at *m*/*z* 605 and 599, respectively. Analogous ions in Fig. 6*B* are observed at *m*/z 757, *m*/*z* 633, and *m*/*z* 627, respectively.

Fig. 6*C* also contains ions *m*/*z* 484, 478, and 425 that identify oleate as a fatty acid substituent. Those ions reflect neutral losses of oleic acid (MLi-282), of Li^+-oleate (MLi-288), and of trimethylamine plus oleic acid (MLi-341), respectively. Palmitate is the other fatty acid substituent, as shown by ions reflecting losses of palmitic acid (*m*/*z* 510), of Li^+-palmitate (*m*/*z* 504), and of trimethylamine plus palmitic acid (*m*/*z* 451). The ion reflecting loss of trimethylamine plus the *sn*-1 substituent is more abundant than the ion reflecting loss of trimethylamine plus the *sn*-2 substituent in GPC lipid-Li^+ CAD spectra (71–73), and the relative abundance of ions *m*/*z* 425 and 451 in Fig. 6*C* indicates that palmitate and oleate are the *sn*-1 and *sn*-2 substituents, respectively.

The most abundant ion in mass spectra of wild-type brain GPC lipids is *m*/*z* 766 (Fig. 5*A*) and represents 16:0/18:1-GPC $[M + Li]^+$, as shown by its tandem spectrum (Fig. 6*C*). Loss of trimethylamine (MLi^+-59) yields the ion *m*/*z* 707, and the ions *m*/*z* 583 (MLi^+-183) and *m*/*z* 577 (MLi^+-189) reflect net loss of $[HPO_4(CH_2)_2N(CH_3)_3]$ or $[LiPO_4(CH_2)_2N(CH_3)_3]$, respectively, and identify the head group (71–73). Fig. 6*C* also contains ions *m*/*z* 484, 478, and 425 that identify oleate as a fatty acid substituent. Those ions reflect neutral losses of oleic acid (MLi-282), of Li^+-oleate (MLi-288), and of trimethylamine plus oleic acid (MLi-341), respectively. Palmitate is the other fatty acid substituent of the parent $[M + Li]^+$ion in Fig. 6*C*, as shown by ions reflecting losses of palmitic acid (*m*/*z* 510), of Li^+-palmitate (*m*/*z* 504), and of trimethylamine plus palmitic acid (*m*/*z* 451). The relative abundance of ions *m*/*z* 425

and 451 in Fig. 6*C* indicates that palmitate and oleate are the *sn*-1 and *sn*-2 substituents, respectively.

An analogous tandem spectrum in Fig. 6*D* identifies the ion at *m*/*z* 794 in Fig. 5*A* as 18:/0/18:1-GPC, as reflected by ions representing neutral losses of trimethylamine plus either the *sn*-1 substituent (MLi^+-341) or the *sn*-2 substituent (MLi^+-343) as free fatty acids at *m*/*z* 453 and *m*/*z* 451, respectively, and by losses of these substituents from $[M + Li]^+$ as free fatty acids (*m*/*z* 512 and *m*/*z* 510) or as Li^+ salts (*m*/*z* 506 and *m*/*z* 504), respectively. Identities of other GPC lipids represented by ions in Fig. 5*A* were similarly determined and include 16:0/16:0-GPC (*m*/*z* 740), 16:0/22:6-GPC (*m*/*z* 812), and 18:0/22:6-GPC (*m*/*z* 840). The tandem spectrum of the ion at *m*/*z* 737 indicates that it represents the sphingomyelin species with stearate as the fatty acid substituent.

Fig. 5*B* is the ESI/MS spectrum of GPC lipid Li^+ adducts from iPLA$_2\beta$-null brain tissue and is virtually identical to that for wild-type brain (Fig. 5*A*). Ions representing the 20:4-containing GPC species at *m*/*z* 788 and 816 are no less abundant in the latter spectrum than in the former, and quantitative measurements with internal standards and normalization to measured lipid phosphorus levels also indicate that 16:/20:4-GPC and 18:0/20:4-GPC are no less abundant in brain from iPLA$_2\beta$-null mice than in brain from wild-type mice. This indicates that the absence of iPLA$_2\beta$ does not result in a deficiency of arachidonate-containing GPC lipids in mouse brain.

Fig. 5*C* is the ESI/MS spectrum of Li^+ adducts of GPC lipids of pancreatic islets from wild-type mice. Most GPC lipid species observed in brain are also observed in islets, although the relative abundance differs between the two tissues, as has also been observed for rat brain and islets (84). Tandem spectra establish that the ion at *m*/*z* 764 represents a mixture of 16:0/18:2-GPC and 16:1/18:1-GPC, that the ion at *m*/*z* 792 represents a mixture of 18:0/18:2-GPC and 18:1/18:1-GPC, and that the ion at *m*/*z* 814 represents predominantly 18:1/20:4-GPC. The relative abundances of those components of the GPC mixture are greater in islets than brain.

In addition, the relative abundances of the arachidonate-containing species 16:0/20:4-GPC (*m*/*z* 788) and 18:0/20:4-GPC (*m*/*z* 816) is notably greater in mouse islets than in brain, as is also the case for rat islets and brain (84). Fig. 5*D* is the ESI/MS spectrum of Li^+ adducts of GPC lipids from islets isolated from iPLA$_2\beta$-null mice and is similar to that for wild-type islets, except for a slightly greater relative abundance of 16:0/22:6-GPC in the iPLA$_2\beta$-null islets. The relative abundances of the ions representing 16:0/20:4-GPC (*m*/*z* 788) and 18:0/20:4-GPC (*m*/*z* 816) are similar in the two spectra and do not indicate a deficiency of 20:4-containing GPC lipids in iPLA$_2\beta$-null islets.

Responses of Wild-type and iPLA$_2$β-Null Mice to Multiple Low Dose Streptozotocin Administration

The phospholipid analyses described above do not indicate an impaired ability to achieve a normal content of arachidonate-containing GPC lipids in brain or islets of iPLA$_2\beta$-null mice, but insulin secretory responses to some stimuli are reduced with islets from iPLA$_2\beta$-null mice compared with those from wild-type mice. These findings support a signaling role for iPLA$_2\beta$ in insulin secretion rather than a housekeeping function in the maintenance of islet phosphatidylcholine composition, but the fasting and fed blood glucose concentrations of iPLA$_2\beta$-null mice do not differ from those of wild-type mice.

This calls into question the importance of any signaling function of iPLA$_2\beta$ in insulin secretion. We wondered whether compensatory mechanisms might override any secretory defect in iPLA$_2\beta$-null islets under normal conditions but imposing a metabolic stress might unmask a latent defect in glucose homeostasis. One such stress that was tested is the administration of multiple low doses of streptozotocin (77).

Streptozotocin is a β-cell toxin, and single large doses are used to induce insulinopenic diabetes in mice and rats by destroying essentially the entire β-cell mass (85). Another protocol involves administration of multiple, small doses of streptozotocin over a period of time (77). This results in a smoldering inflammatory process that reduces β-cell number but leaves a substantial functional β-cell mass. This state is somewhat analogous to type II diabetes, in which some β-cell function is preserved, but insulin secretion is sufficiently impaired to result in defects in glucose homeostasis. This model has been used to examine effects of gene disruption on sensitivity to diabetogenic stimuli (77).

Wild-type and iPLA$_2\beta$-null mice were thus subjected to five daily intraperitoneal injections of streptozotocin (40 mg/kg) and then maintained on a standard laboratory chow diet, and their blood glucose concentrations were determined after an overnight fast at various intervals. Wild-type mice developed a modest increase in fasting blood glucose concentrations that rose progressively in the period 1–7 weeks after streptozotocin administration (Fig. 7*A*). The iPLA$_2\beta$-null mice experienced a significantly greater increase in fasting blood glucose concentration than did wild-type mice at 1 week and experienced greater further increases in fasting blood glucose concentration than did wild-type mice at every tested interval up to 7 weeks after injection. This is compatible with an impaired insulin secretory reserve in iPLA$_2\beta$-null islets that is latent under unstressed conditions but unmasked by reducing β-cell mass.

Fig. 7*B* illustrates that fasting blood insulin concentrations decline after streptozotocin administration, and the falling insulin levels indicate that streptozotocin did injure β-cells and impair insulin secretion. The insulin levels are quite variable, as is often the case with mouse blood insulin measurements (69), and do not differ significantly between wild-type and iPLA$_2\beta$-null mice. Nonetheless, the significantly higher fasting glucose levels of the latter compared with the former reflect the expected impairment of insulin secretion after streptozotocin administration.

The fact that different insulin values are not observed between wild-type and iPLA$_2\beta$-null mice is attributable partly to the variability in mouse blood insulin measurements, but, more importantly, to the fact that, if there were no impairment of insulin secretion in the iPLA$_2\beta$-null mice, one would expect them to exhibit higher insulin values than wild-type mice because the former have higher blood glucose concentrations.

Similar observations have been made with genetically modified mice with altered islet lipoprotein lipase (LPL) expression (69). Although these mice developed hyperglycemia after challenge, there were no differences in blood insulin concentration between these animals and their normoglycemic wild-type littermates. The failure to detect higher insulin levels in the setting of hyperglycemia was taken to reflect defective insulin secretion, which was confirmed using isolated islets (69).

There are a number of other examples in which there is a discrepancy between blood insulin levels and genetic perturbations of β-cell function that disturb glucose homeostasis in mice, and some of them are summarized in “Discussion.” As discussed further below, no differences in insulin-tolerance testing responses were observed between wild-type and iPLA$_2\beta$-null mice fed a regular diet.

Responses of Wild-type and iPLA$_2\beta$-Null Mice Fed a High Fat Diet

Another metabolic stress that was tested is maintaining the mice on a high fat diet, which is also a known diabetogenic stimulus (86) that can result in both insulin resistance (87) and attenuation of insulin secretion (88). Wild-type and iPLA$_2\beta$-null mice were thus placed on a high fat diet or regular chow at 8 weeks of age and maintained on the diet for 6 months. At the

end of that period, glucose tolerance testing (GTT) and insulin tolerance testing (ITT) were performed.

Compared with mice maintained on regular chow, both wild-type (Fig. 8*A*) and iPLA$_2\beta$-null mice (Fig. 8*B*) fed a high fat diet developed a significant increase in fasting blood glucose concentrations, as reflected by the time 0 points in the GTT curves in Fig. 8. In response to an intraperitoneal glucose load, wild-type mice maintained on the high fat diet were less glucose tolerant than those fed regular chow, as reflected by an increase in the area under the glucose concentration *versus* time curve (89) from 213 ± 4.3 area units (au) for mice fed standard chow to 318 ± 35 au for mice fed the high fat diet ($p = 0.0035$), which represented a difference in areas under the two GTT curves of 105 au (Fig. 9*A*).

The iPLA$_2\beta$-null mice fed the high fat diet experienced a greater deterioration in glucose tolerance than did wild-type mice, as reflected by a significant increase in the area under the GTT curve from 200 ± 8.6 au for mice fed standard chow to 411 ± 27 au for mice fed the high fat diet ($p = 0.0002$). This represented a difference in areas under the two GTT curves of 211 au for iPLA$_2\beta$-null mice, a value twice as great that for wild-type mice (Fig. 9*A*).

Although the fasting blood glucose concentrations at time 0 of the GTT did not differ between wild-type (112 ± 3.0 mg/dl) and iPLA$_2\beta$-null (112 ± 3.5 mg/dl) mice that had been fed a high fat diet, the mean blood glucose values after intraperitoneal glucose administration were significantly ($p = 0.022$) higher for iPLA$_2\beta$-null (244 ± 19 mg/dl) than for wild-type (189 ± 13 mg/dl) mice, as were the increases in glucose concentrations (132 ± 19 mg/dl for iPLA$_2\beta$-null mice and 78 ± 13 mg/dl for wild-type mice, respectively, $p = 0.022$). This indicates that iPLA$_2\beta$-null mice experience a greater deterioration in glucose tolerance when fed a high fat diet than do wild-type mice and provides another example of a metabolic stress that exposes a latent defect in glucose homeostasis in iPLA$_2\beta$-null mice that is not apparent in the basal state.

For wild-type mice maintained on a regular diet, intraperitoneal glucose administration resulted in a rise in mean blood insulin concentration from 323 ± 48 pg/ml to 781 ± 129 pg/ml, and the corresponding values for iPLA$_2\beta$-null mice were 296 ± 47 and 644 ± 6 pg/ml, respectively (Table 1). Wild-type mice fed a high fat diet experienced an increase in fasting blood insulin concentration (to 1080 ± 143 pg/ml) relative to those fed regular chow, and their insulin levels rose to a mean of 2600 ± 420 pg/ml after intraperitoneal glucose administration. The corresponding values for iPLA$_2\beta$-null mice were 990 ± 129 and 2330 ± 227 pg/ml, respectively (Table 1).

The fact that mice fed a high fat diet exhibit higher blood insulin concentrations than do those fed normal chow likely reflects an increase in insulin resistance, and the fact that blood glucose levels also rise reflects an insulin secretory defect, consistent with previously reported effects of a high fat diet on glucose homeostasis in mice (86–88).

Although there is a trend for iPLA$_2\beta$-null mice in both dietary groups to exhibit lower blood insulin levels than wild-type mice before and after intraperitoneal glucose administration, this was not statistically significant because of the magnitude of the variability in measured insulin levels. Given that the iPLA$_2\beta$-null mice developed higher blood glucose concentrations than wild-type mice after intraperitoneal glucose admin istration, they would be expected to have higher blood insulin concentrations if their insulin secretory defect were not more severe that that of wild-type mice, as discussed above and elsewhere (69).

Significant differences can be observed in blood insulin/glucose ratios in glucose tolerance testing in genetically modified mice with insulin secretory defects compared with wild-type mice even when absolute insulin concentrations do not differ significantly (90), and this also

is the case for iPLA$_2\beta$-null mice fed a high fat diet (Fig. 9*B*). These mice exhibit significantly lower blood insulin/glucose ratios than do wild-type mice fed a high fat diet at 30 min after intraperitoneal glucose administration (Fig. 9*B*). For wild-type mice, the high fat diet results in more than a doubling of the blood insulin/glucose ratio achieved in response to intraperitoneal glucose challenge compared with mice fed a regular diet, which presumably represents a compensatory response to increased insulin resistance induced by high fat feeding. An increase in the stimulated blood insulin/glucose ratio also occurs in iPLA$_2\beta$-null mice fed a high fat diet, but the magnitude of the rise is significantly less than that for wild-type mice (Fig. 9*B*).

Interestingly, iPLA$_2\beta$-null mice fed a high fat diet exhibited greater sensitivity to exogenous insulin than did wild-type mice fed a high fat diet, as reflected by significantly lower blood glucose concentrations in iPLA$_2\beta$-null than in wild-type mice at 30 min ($p = 0.011$), 60 min ($p = 0.017$), and 120 min ($p = 1.5 \times 10^{-9}$) after insulin administration (Fig. 10). No differences in insulin tolerance testing responses were observed between wild-type and iPLA$_2\beta$-null mice fed regular chow. This suggests that iPLA$_2\beta$-null mice are less sensitive than wild-type mice to the high fat diet-induced increase in insulin resistance. The greater glucose intolerance of iPLA$_2\beta$-null mice compared with wild-type mice fed a high fat diet is thus likely to reflect a more pronounced impairment in insulin secretory responses.

To further examine this possibility, pancreatic islets were isolated from wild-type and iPLA$_2\beta$-null mice that had been fed a high fat diet, and their insulin secretory responses were studied *ex vivo* (Fig. 11). Compared with islets isolated from wild-type mice fed a regular diet (Fig. 4), islets from wild-type mice fed a high fat diet exhibited exaggerated insulin secretory responses to 8 and 20 mM D-glucose in the absence or presence of 2.5 μM forskolin (Fig. 11), which is consistent with the higher blood insulin levels observed in the high fat fed animals that presumably reflect compensation for diet-induced insulin resistance (Table 1). The *ex vivo* insulin secretory responses of islets from iPLA$_2\beta$-null mice fed a high fat diet were even more impaired compared with wild-type islets (Fig. 11) than were those from mice fed a regular diet (Fig. 4).

DISCUSSION

We have generated iPLA$_2\beta$-null mice by homologous recombination that have previously been reported to exhibit the phenotypic abnormalities of reduced male fertility associated with impaired production and motility of spermatozoa (66) and defective signaling in macrophages (38). We confirm here that no iPLA$_2\beta$ mRNA is expressed in any tissue examined from iPLA$_2\beta$-null animals of any age, including pancreatic islets and brain, although proteins that cross-react with anti-bodies to iPLA$_2\beta$ are frequently observed in brain and other tissues. In addition, an iPLA$_2\beta$ mutant protein that lacks sequence encoded by exon 9 of the *iPLA$_2\beta$* gene has been expressed in a baculovirus-Sf9 cell system, purified by immobilized metal affinity chromatography, and demonstrated not to exhibit iPLA$_2\beta$ catalytic activity.

It has been proposed that iPLA$_2\beta$ plays the housekeeping roles of providing 2-lysophosphatidylcholine (LPC) acceptors for incorporating arachidonic acid into PC (22–25) and of maintaining membrane phospholipid homeostasis by degrading excess PC (28,29), This could have important implications for pancreatic islet function because islets contain the highest fraction of arachidonate esterified in their phospholipids, including phosphatidylcholine, of any known tissue (81,84), and the physical properties of such phospholipids are likely to have an important influence on fusion of secretory granule and plasma membranes (84,92), which is the final event in insulin exocytosis.

Nonetheless, we observe a PC composition in pancreatic islets and brain of iPLA$_2\beta$-null mice that is similar or identical to that of wild-type mice, as is also the case with the PC composition of testes from iPLA$_2\beta$-null and wild-type mice (66). In particular, there is no deficiency in arachidonic acid-containing PC species in any of these tissues from iPLA$_2\beta$-null mice. Our ESI/MS findings that the PC content and composition of pancreatic islets from iPLA$_2\beta$-null and wild-type mice are virtually identical are consistent with the lack of effects of pharmacologic inhibition of iPLA$_2\beta$ activity (50,76) or molecular biologic manipulation of iPLA$_2\beta$ expression (59,60) on these parameters in insulinoma cells and islets from rats. Neither stable over-expression (59) nor suppression (60) of iPLA$_2\beta$ expression in INS-1 insulinoma cells results in a significant change in their PC content or composition or rates of arachidonic acid incorporation into PC.

Although we find no evidence that iPLA$_2\beta$ plays the proposed housekeeping roles in PC homeostasis (28,29) and remodeling (23–25) in pancreatic islet β-cells, iPLA$_2\beta$ is widely expressed and might have multiple functions that vary among tissues and cell types, perhaps dependent in part on which splice variants (42–45) and proteolytic processing products (31, 50,70) of iPLA$_2\beta$ are expressed in a given cell and on what interacting proteins (71) are present in the cell compartment (59,93) in which the iPLA$_2\beta$ isoform resides.

Our findings do indicate that pancreatic islets isolated from iPLA$_2\beta$-null mice exhibit impaired insulin secretory responses to stimulatory concentrations of D-glucose and forskolin compared with those from wild-type mice, and this is consistent with other evidence that iPLA$_2\beta$ participates in insulin secretion. Pharmacologic inhibition of iPLA$_2\beta$ with BEL impairs stimulated insulin secretion from rat (47) and human (81) pancreatic islets and from several clonal β-cell lines (48–50).

Because BEL affects several targets in addition to iPLA$_2\beta$ (17,18,20,21,57,58,94), it is important to use molecular biologic manipulation of iPLA$_2\beta$ activity to complement pharmacologic findings. Stable overexpression of iPLA$_2\beta$ in INS-1 insulinoma cells amplifies stimulated insulin secretion (59), and transient (41) or stable (60) suppression of iPLA$_2\beta$ expression impairs insulin secretion, consistent with the reduced secretory responses of iPLA$_2\beta$-null islets reported here.

In glucose-induced insulin secretion, glucose enters β-cells via GLUT-II transporters and is phosphorylated by glucokinase, which results in generation of metabolic signals that include increased [ATP]/[ADP] (95). This inactivates plasma membrane (PM) ATP-sensitive K^+ channels (K_{ATP}) (96), causing membrane depolarization, activation of PM voltage-operated Ca^{2+} channels (VOCC), Ca^{2+} influx, and a rise in [Ca^{2+}] (97) that triggers insulin exocytosis through Ca^{2+}-sensitive effectors, including Ca^{2+}/calmodulin-dependent protein kinase IIβ (98).

Phospholipid hydrolysis catalyzed by iPLA$_2\beta$ and accumulation of the products nonesterified arachidonate and LPC in β-cell membranes (99–102) have been proposed to amplify the glucose-induced rise in β-cell [Ca^{2+}] and insulin secretion by several mechanisms. These include facilitating Ca^{2+} entry (99,102), perhaps by arachidonate effects on VOCC (103), effects of LPC and arachidonate on K_{ATP} (104), effects of an arachidonate 12-lipoxygenase product on a PM Na^+/K^+-ATPase (45), and effects of LPC (36) on PM store-operated cation channels (105).

Although abnormal insulin secretory responses are demonstrable with pancreatic islets isolated from iPLA$_2\beta$-null mice, these mice do not exhibit fasting or fed hyperglycemia under ordinary circumstances and gain weight at the same rate as wild-type littermates. The failure to observe overt hyperglycemia despite defective insulin secretory responses of isolated islets is also observed in mice in which the gene encoding the Kir6.2 component of the K_{ATP} channel is

disrupted by homologous recombination (61). Glucose intolerance is induced in the Kir6.2-null mice by imposing the metabolic stress of a high fat diet or the development of obesity, and this is associated with exacerbation of insulin secretory defects (62,63).

Prolonged feeding of a high fat diet also induces glucose intolerance in iPLA$_2\beta$-null mice that is more severe than that induced in wild-type mice, and this does not appear to be attributable to a more severe deterioration in insulin-sensitivity because iPLA$_2\beta$-null mice are more responsive to exogenous insulin administration than are wild-type mice after 6 months of high dietary fat intake, as reflected by the magnitude of the hypoglycemic response. The observation that iPLA$_2\beta$-null mice develop more severe hyperglycemia than do wild-type mice after administration of multiple low doses of streptozotocin also suggests that the islet secretory reserve is reduced in iPLA$_2\beta$-null mice and that this results in an impaired ability to compensate for metabolic stresses.

Although there is a trend for blood insulin levels to be lower in iPLA$_2\beta$-null mice than in wild-type mice in glucose-tolerance testing studies, the large variability in measured insulin levels prevents the difference from achieving statistical significance. We nonetheless believe that the more severe impairment of glucose tolerance of iPLA$_2\beta$-null mice compared with wild-type mice fed a high fat diet is attributable to more severely impaired insulin secretion. Mouse blood insulin levels are not always a reliable indicator of β-cell function *in vivo* (*e.g.* Refs. 69,83, 90,91,105), in part because of great analytical variability to which a mouse red cell insulinase is thought to contribute (69).

In addition, blood insulin levels must be interpreted in the context of blood glucose levels and cannot be compared directly in absolute concentrations without considering glucose levels. The blood insulin/glucose concentration ratio achieved 30 min after intraperitoneal glucose administration was significantly lower in iPLA$_2\beta$-null than in wild-type mice that had been fed a high fat diet, and this ratio has also been observed to be lower in other genetically modified mice with an insulin secretory defect compared with wild-type mice even when the absolute blood insulin concentrations do not differ significantly between the groups (90).

Because iPLA$_2\beta$-null mice fed a high fat diet develop higher blood glucose concentrations than do wild-type mice after intraperitoneal glucose administration, they would be expected to have higher blood insulin concentrations if their insulin secretory defect were not more severe that that of wild-type mice (69,83,90,91,105). The fact that the iPLA$_2\beta$-null mice have blood insulin levels that are less than or equal to those of wild-type mice, despite the fact that the iPLA$_2\beta$-null mice have higher glucose levels in GTT studies after high fat feeding, implies that their insulin secretory defect is more severe than that of wild-type mice (69,83,90,91,105).

There are many examples in which there are discrepancies between measured blood insulin levels and genetic perturbations of β-cell function that disturb glucose homeostasis in mice. As discussed above, β-cell-specific disruption of the lipoprotein lipase (*LPL*) gene results in mice that have impaired glucose tolerance, but their blood insulin levels do not differ significantly from those of wild-type mice during GTT studies (69). Nonetheless, islets isolated from β-cell-specific LPL knock-out mice exhibit impaired insulin secretory responses *in vitro*; the mice exhibit normal insulin sensitivity in insulin-tolerance tests; and their impaired glucose tolerance is attributable to impaired insulin secretion despite measured blood insulin levels that do not differ from those of wild-type mice (69).

Similarly, β-cell specific knock-out of the ARNT transcription factor gene results in male mice that have impaired glucose tolerance on GTT studies, but their blood insulin levels are indistinguishable from those of wild-type mice during such studies (91). Nonetheless, islets isolated from the male β-cell-specific ARNT-null mice have defective insulin secretory responses, and their impaired glucose tolerance is attributable to impaired insulin secretion,

even though their measured blood insulin levels are not different from those of wild-type mice (91).

Moreover, β-cell-specific knock-out of the Hnf1β transcription factor gene results in mice that have impaired glucose tolerance on GTT studies (90). Their absolute blood insulin levels are nonetheless indistinguishable from those of wild-type mice during such studies, although islets isolated from the β-cell-specific Hnf1β-null mice have defective insulin secretory responses, and their glucose intolerance is also attributable to impaired insulin secretion (90). This is also reflected by the lower blood insulin/glucose concentration ratios during the GTT for the genetically modified compared with wild-type mice (90).

In addition, 8-month-old female transgenic mice that over-express the Sir2 protein deacetylase specifically in β-cells have significantly better glucose tolerance on GTT studies than do wild-type mice, but their glucose-induced rise in blood insulin levels is not statistically different from that of wild-type mice during such studies (83). Nonetheless, glucose-stimulated insulin release from their perfused pancreata is significantly greater than that for wild-type mice, and their improved glucose tolerance is attributable to augmented insulin secretion despite the fact that measured blood insulin levels are not elevated (83).

Our findings are thus quite similar to those of each of the four studies of glucose homeostasis in genetically modified mice just described (69,83,90,91,105). Disruption of the *iPLA$_2\beta$* gene results in mice that exhibit impaired glucose tolerance after exposure to stressors that include administration of multiple low doses of streptozotocin or a high fat diet. There is a trend for the iPLA$_2\beta$-null mice to exhibit lower blood insulin levels than do wild-type mice after intraperitoneal glucose administration, but this does not achieve statistical significance because of the large variability in measured blood insulin levels. Nonetheless, islets isolated from the iPLA$_2\beta$-null mice exhibit impaired insulin secretory responses *ex vivo*; this insulin secretory impairment compared with wild-type islets is exaggerated with islets from iPLA$_2\beta$-null mice fed a high fat diet; the results of insulin tolerance testing indicate that iPLA$_2\beta$-null mice do not have reduced insulin sensitivity; and their reduced glucose tolerance thus appears to result from inadequate insulin secretion.

These findings thus contribute to a large body of evidence that iPLA$_2\beta$ plays a role in stimulated insulin secretion and indicate that homozygous *iPLA$_2\beta$* gene disruption produces phenotypic abnormalities in several tissues and cells that include pancreatic islets in addition to testes (66) and macrophages (38).

Acknowledgements

We thank Sheng Zhang and Min Tan for excellent technical assistance and Dr. Richard Gross for the gift of iPLA$_2\beta$ antibody 506.

References

1. Six DA, Dennis EA. Biochim Biophys Acta 2000;1488:1–19. [PubMed: 11080672]
2. Ma Z, Turk J. Prog Nucleic Acids Res Mol Biol 2001;67:1–33.
3. Brash AR. J Clin Investig 2001;107:1339–1345. [PubMed: 11390413]
4. Radu CG, Yang LV, Riedinger M, Au M, Witte ON. Proc Natl Acad Sci U S A 2004;101:245–250. [PubMed: 14681556]
5. Murphy RC, Sala A. Methods Enzymol 1990;187:90–98. [PubMed: 2233370]
6. Gijon MA, Spencer DM, Kaiser AL, Leslie CC. J Cell Biol 1999;145:1219–1232. [PubMed: 10366595]
7. Underwood KW, Song C, Kriz RW, Chang XJ, Knopf JL, Lin LL. J Biol Chem 1998;273:21926–21932. [PubMed: 9705332]

8. Pickard RT, Strifler BA, Kramer RM, Sharp JD. J Biol Chem 1999;274:8823–8831. [PubMed: 10085124]
9. Song C, Chang XJ, Bean KM, Proia MS, Knopf JL, Kriz RW. J Biol Chem 1999;274:17063–17067. [PubMed: 10358058]
10. Ohto T, Uozumi N, Hirabayashi T, Shimizu T. J Biol Chem 2005;280:24576–24583. [PubMed: 15866882]
11. Tang J, Kriz RW, Wolfman N, Shaffer M, Seehra J, Jones SS. J Biol Chem 1997;272:8567–8575. [PubMed: 9079687]
12. Balboa MA, Balsinde J, Jones SS, Dennis EA. J Biol Chem 1997;272:8576–8580. [PubMed: 9079688]
13. Ma Z, Ramanadham S, Kempe K, Chi XS, Ladenson J, Turk J. J Biol Chem 1997;272:11118–11127. [PubMed: 9111008]
14. Hazen SL, Zupan LA, Weiss RH, Getman DP, Gross RW. J Biol Chem 1991;266:7227–7232. [PubMed: 2016324]
15. Balsinde J, Dennis EA. J Biol Chem 1997;272:16069–16072. [PubMed: 9195897]
16. Ma Z, Ramanadham S, Hu Z, Turk J. Biochim Biophys Acta 1998;1391:384–400. [PubMed: 9555100]
17. Balsinde J, Dennis EA. J Biol Chem 1996;271:6758–6765. [PubMed: 8636097]
18. Mancuso DJ, Jenkins CM, Gross RW. J Biol Chem 2000;275:9937–9945. [PubMed: 10744668]
19. Tanaka H, Takeya R, Sumimoto H. Biochem Biophys Res Commun 2000;272:320–326. [PubMed: 10833412]
20. van Tienhoven M, Atkins J, Li Y, Glynn P. J Biol Chem 2002;277:20942–20948. [PubMed: 11927584]
21. Jenkins CM, Mancuso DJ, Yan W, Sims HF, Gibson B, Gross RW. J Biol Chem 2004;279:48968–48975. [PubMed: 15364929]
22. Balsinde J. Biochem J 2002;364:695–702. [PubMed: 12049633]
23. Balsinde J, Balboa MA. Cell Signal 2005;17:1052–1062. [PubMed: 15993747]
24. Balsinde J, Bianco ID, Ackermann EJ, Conde-Frieboes K, Dennis EA. Proc Natl Acad Sci U S A 1995;92:8527–8531. [PubMed: 7667324]
25. Balsinde J, Balboa MA, Dennis EA. J Biol Chem 1997;272:29317–29321. [PubMed: 9361012]
26. Lands, WEM.; Crawford, CG. The Enzymes of Biological Membranes. Plenum Press; New York: 1997.
27. Chilton FH, Fonteh AN, Surette ME, Triggiani M, Winkler JD. Biochim Biophys Acta 1996;1299:1–15. [PubMed: 8555241]
28. Baburina I, Jackowski S. J Biol Chem 1999;274:9400–9408. [PubMed: 10092620]
29. Barbour SE, Kapur A, Deal CL. Biochim Biophys Acta 1999;1439:77–88. [PubMed: 10395967]
30. Akiba S, Mizunaga S, Kume K, Hayama M, Sato T. J Biol Chem 1999;274:19906–19912. [PubMed: 10391937]
31. Atsumi G, Murakami M, Kojima K, Hadano A, Tajima M, Kudo I. J Biol Chem 2000;275:18248–18258. [PubMed: 10747887]
32. Jenkins CM, Han X, Mancuso DJ, Gross RW. J Biol Chem 2002;277:32807–32814. [PubMed: 12089145]
33. Seegers HC, Gross RW, Boyle WA. J Pharmacol Exp Ther 2002;302:918–923. [PubMed: 12183647]
34. Perez R, Melero R, Balboa MA, Balsinde J. J Biol Chem 2004;279:40385–40391. [PubMed: 15252038]
35. Yellaturu CR, Rao GN. J Biol Chem 2003;278:43831–43837. [PubMed: 12928445]
36. Smani T, Zakharov SI, Csutora P, Leno E, Trepakova ES, Bolotina VM. Nat Cell Biol 2004;6:113–120. [PubMed: 14730314]
37. Martinson BD, Albert CJ, Corbett JA, Wysolmerski RB, Ford DA. J Lipid Res 2003;44:1686–1691. [PubMed: 12810819]
38. Moran JM, Buller RM, McHowat J, Turk J, Wohltmann M, Gross RW, Corbett JA. J Biol Chem 2005;280:28162–28168. [PubMed: 15946940]
39. Guo Z, Su W, Ma Z, Smith GM, Gong MC. J Biol Chem 2003;278:1856–1863. [PubMed: 12421808]
40. Balboa MA, Saez Y, Balsinde J. J Immunol 2003;170:5276–5280. [PubMed: 12734377]

41. Song K, Zhang X, Zhao C, Ang NT, Ma ZA. Mol Endocrinol 2005;19:504–515. [PubMed: 15471944]
42. Larsson Forsell PK, Kennedy BP, Claesson HE. Eur J Biochem 1999;262:575–585. [PubMed: 10336645]
43. Ma Z, Wang X, Nowatzke W, Ramanadham S, Turk J. J Biol Chem 1999;274:9607–9616. [PubMed: 10092647]
44. Larsson PK, Claesson HE, Kennedy BP. J Biol Chem 1998;273:207–214. [PubMed: 9417066]
45. Owada S, Larsson O, Arkhammar P, Katz AI, Chibalin AV, Berggren PO, Bertorello AM. J Biol Chem 1999;274:2000–2008. [PubMed: 9890957]
46. Simonsson E, Ahren B. Int J Pancreatol 2000;27:1–11. [PubMed: 10811018]
47. Ramanadham S, Gross RW, Han X, Turk J. Biochemistry 1993;32:337–346. [PubMed: 8418854]
48. Ramanadham S, Wolf MJ, Jett PA, Gross RW, Turk J. Biochemistry 1994;33:7442–7452. [PubMed: 8003509]
49. Ramanadham S, Wolf MJ, Li B, Bohrer A, Turk J. Biochim Biophys Acta 1997;1344:153–164. [PubMed: 9030192]
50. Ramanadham S, Song H, Hsu FF, Zhang S, Crankshaw M, Grant GA, Newgard CB, Bao S, Ma Z, Turk J. Biochemistry 2003;42:13929–13940. [PubMed: 14636061]
51. Ramanadham S, Ma Z, Arita H, Zhang S, Turk J. Biochim Biophys Acta 1998;1390:301–312. [PubMed: 9487151]
52. Su X, Mancuso DJ, Bickel PE, Jenkins CM, Gross RW. J Biol Chem 2004;279:21740–21748. [PubMed: 15024020]
53. Shirai Y, Balsinde J, Dennis EA. Biochim Biophys Acta 2005;1735:119–129. [PubMed: 15967714]
54. Akiba S, Sato T. Biol Pharm Bull 2004;27:1174–1178. [PubMed: 15305016]
55. Larsson Forsell PK, Runarsson G, Ibrahim M, Bjorkholm M, Claesson HE. FEBS Lett 1998;434:295–299. [PubMed: 9742941]
56. Murakami M, Kambe T, Shimbara S, Kudo I. J Biol Chem 1999;274:3103–3115. [PubMed: 9915849]
57. Daniels S, Cooney E, Sofia M, Chakravarty P, Katzenellenbogen J. J Biol Chem 1983;258:15046–15053. [PubMed: 6654902]
58. Fuentes L, Perez R, Nieto ML, Balsinde J, Balboa MA. J Biol Chem 2003;278:44683–44690. [PubMed: 12952946]
59. Ma Z, Ramanadham S, Wohltmann M, Bohrer A, Hsu FF, Turk J. J Biol Chem 2001;276:13198–13208. [PubMed: 11278673]
60. Bao S, Bohrer A, Ramanadham S, Jin W, Zhang S, Turk J. J Biol Chem 2006;281:187–198. [PubMed: 16286468]
61. Miki T, Nagashima K, Tashiro F, Kotake K, Yoshitomi H, Tamamoto A, Gonoi T, Iwanaga T, Myazaki J, Seino S. Proc Natl Acad Sci 1998;95:10402–10496. [PubMed: 9724715]
62. Seino S, Iwanaga T, Nagashima K, Miki T. Diabetes 2000;49:311–318. [PubMed: 10868950]
63. Remedi MS, Koster JC, Markova K, Seino S, Miki T, Patton BL, McDaniel ML, Nichols CG. Diabetes 2000;53:3159–3167. [PubMed: 15561946]
64. Bonventre JV, Huang Z, Taheri MR, O'Leary E, Li E, Moskowitz MA, Sapirstein A. Nature 1997;390:622–625. [PubMed: 9403693]
65. Uozumi N, Kume K, Nagase T, Nakatani N, Ishii S, Tashiro F, Komagata Y, Maki K, Ikuta K, Ouchi Y, Miyazaki J, Shimizu T. Nature 1997;390:618–622. [PubMed: 9403692]
66. Bao S, Miller DJ, Ma Z, Wohltmann M, Eng G, Ramanadham S, Moley K, Turk J. J Biol Chem 2004;279:38194–38200. [PubMed: 15252026]
67. Hallberg A. Biochim Biophys Acta 1984;796:328–335. [PubMed: 6391554]
68. McDaniel ML, Colca JR, Kotagal N, Lacy PE. Methods Enzymol 1983;98:182–200. [PubMed: 6366468]
69. Pappan KL, Pan Z, Kwon G, Marshall CA, Coleman T, Goldberg IJ, McDaniel ML, Semenkovich CF. J Biol Chem 2005;280:9023–9029. [PubMed: 15637076]
70. Song H, Hecimovic S, Goate A, Hsu FF, Bao S, Vidavsky I, Ramanadham S, Turk J. J Am Soc Mass Spectrom 2004;12:1780–1793. [PubMed: 15589755]

71. Wang Z, Ramanadham S, Ma ZA, Bao S, Mancuso DJ, Gross RW, Turk J. J Biol Chem 2005;280:6840–6849. [PubMed: 15576376]
72. Hsu FF, Bohrer A, Turk J. J Am Soc Mass Spectrom 1998;9:516–526. [PubMed: 9879366]
73. Hsu FF, Turk J. J Am Soc Mass Spectrom 2001;12:1036–1043.
74. Hsu FF, Turk J. J Am Soc Mass Spectrom 2003;14:352–363. [PubMed: 12686482]
75. Nowatzke W, Ramanadham S, Ma Z, Hsu FF, Bohrer A, Turk J. Endocrinology 1998;139:4073–4085. [PubMed: 9751485]
76. Ramanadham S, Hsu FF, Bohrer A, Ma Z, Turk J. J Biol Chem 1999;274:13915–13927. [PubMed: 10318801]
77. Bleich D, Chen S, Zipser B, Sun D, Funk CD, Nadler JL. J Clin Invest 1999;103:1431–1436. [PubMed: 10330425]
78. Cheverud JM, Ehrich TH, Hrbek T, Kenney JP, Pletscher LS, Semenkovich CF. Diabetes 2004;53:3328–3336. [PubMed: 15561968]
79. Yang HC, Mosior M, Ni B, Dennis EA. J Neurochem 1999;73:1278–1287. [PubMed: 10461922]
80. Hsu FF, Bohrer A, Turk J. Biochim Biophys Acta 1998;1392:202–216. [PubMed: 9630631]
81. Ramanadham S, Bohrer A, Gross RW, Turk J. Biochemistry 1993;32:13499–13509. [PubMed: 8257685]
82. Mancuso DJ, Abendschein DR, Jenkins CM, Han X, Saffitz JE, Schuessler RB, Gross RW. J Biol Chem 2003;278:22231–22236. [PubMed: 12719436]
83. Moynihan KA, Grimm AA, Plueger MM, Bernal-Mizrachi E, Ford E, Cras-Meneur C, Permutt MA, Imai S. Cell Metab 2005;2:105–117. [PubMed: 16098828]
84. Ramanadham S, Hsu FF, Bohrer A, Nowatzke W, Ma Z, Turk J. Biochemistry 1998;37:4533–4567.
85. Eizrik DL, Strandell E, Bendtzen K, Sandler S. Diabetes 1998;37:916–919.
86. Surwit RS, Kuhn M, Cochrane C, McCubbin JA, Feinglos MN. Diabetes 1988;37:1163–1167. [PubMed: 3044882]
87. Collins S, Martin TL, Surwit RS, Robidoux J. Physiol Behav 2004;81:243–248. [PubMed: 15159170]
88. Wencel HE, Smothers C, Opara EC, Kuhn CM, Feinglos MN, Surwit RS. Physiol Behav 1995;57:1215–1220. [PubMed: 7652047]
89. Kubota N, Terauchi Y, Kubota T, Kumagai H, Itoh S, Satoh H, Yano W, Ogata H, Tokuyama I, Mineyama T, Ishikawa M, Moroi M, Sugi K, Yamauchi T, Ueki K, Tobe K, Noda T, Nagai R, Kadowaki T. J Biol Chem 2006;281:8748–8755. [PubMed: 16431926]
90. Wang L, Coffinier C, Thomas MK, Gresh L, Eddu G, Manor T, Levitsky LL, Yaniv M, Rhoads DB. Endocrinology 2004;145:3941–3949. [PubMed: 15142986]
91. Gunton JE, Kulkarni RN, Yim S, Okada T, Hawthorne WJ, Tseng YH, Roberson RS, Ricordi C, O'Connell PJ, Gonzalez FJ, Kahn CR. Cell 2005;122:337–349. [PubMed: 16096055]
92. Han X, Ramanadham S, Turk J, Gross RW. Biochim Biophys Acta 1998;1414:95–107. [PubMed: 9804907]
93. Bao S, Jin C, Zhang S, Turk J, Ma Z, Ramanadham S. Diabetes 2004;53 (Suppl 1):S186–S189. [PubMed: 14749286]
94. Song H, Ramanadham S, Bao S, Hsu FF, Turk J. Biochemistry 2006;45:1061–1073. [PubMed: 16411783]
95. Meglasson MD, Matschinsky FM. Diabetes Metab Rev 1986;2:163–214. [PubMed: 2943567]
96. Cook DL, Satin LS, Ashford ML, Hales CN. Diabetes 1988;37:495–498. [PubMed: 2452107]
97. Arkhammar P, Nilsson T, Rorsman P, Berggren PO. J Biol Chem 1987;262:5448–5454. [PubMed: 2437108]
98. Easom RA. Diabetes 1999;48:675–684. [PubMed: 10102681]
99. Wolf BA, Pasquale SM, Turk J. Biochemistry 1991;30:6372–6379. [PubMed: 1905151]
100. Wolf BA, Colca JR, Comens PG, Turk J, McDaniel ML. J Biol Chem 1986;261:16284–16287. [PubMed: 3023346]
101. Turk J, Mueller M, Bohrer A, Ramanadham S. Biochim Biophys Acta 1992;1125:280–291. [PubMed: 1596516]

102. Ramanadham S, Gross R, Turk J. Biochem Biophys Res Commun 1992;184:647–653. [PubMed: 1575739]

103. Vacher P, McKenzie J, Dufy B. Am J Physiol 1989;257:E203–E211. [PubMed: 2504050]

104. Eddlestone GT. Am J Physiol 1995;268:C181–C190. [PubMed: 7840146]

105. Roe MW, Worley JF 3rd, Qian F, Tamarina N, Mittal AA, Dralyuk F, Blair NT, Mertz RJ, Philipson LH, Dukes ID. J Biol Chem 1998;273:10402–10410. [PubMed: 9553098]

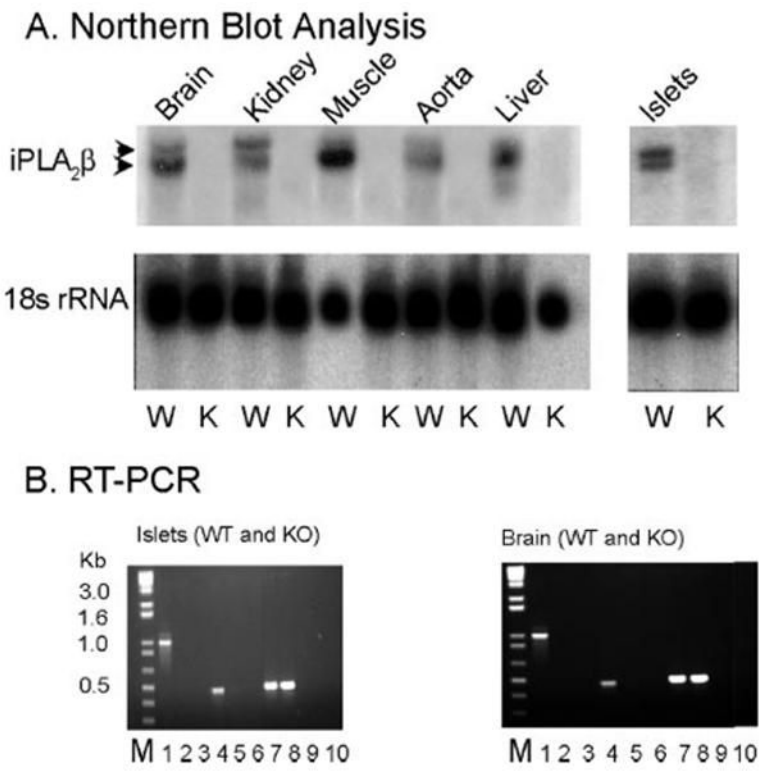

FIGURE 1. Expression of iPLA$_2\beta$ mRNA in tissues of wild-type and iPLA$_2\beta$-null mice

A represents Northern blot analyses of total RNA from wild-type (*WT* or *W*) and iPLA$_2\beta$-null (*KO* or *K*) mouse brain, kidney, skeletal, muscle, aorta, liver, and isolated pancreatic islets. The *upper panels* were probed for iPLA$_2\beta$ mRNA, and the *lower panels* were probed for 18 S ribosomal RNA. *B* depicts analyses of products from RT-PCR amplification of iPLA$_2\beta$ mRNA fragments using total RNA isolated from pancreatic islets and brain as template and two different sets of primers. *Lane M* represents molecular weight standards. *Lanes 1*, *4*, and *7* represent WT tissue, and *lanes 2*, *5*, and *8* represent iPLA$_2\beta$-knock-out (KO) tissues. *Lanes 3*, *6*, *9*, and *10* represent control reactions in which no template was added. In *lanes 1–3*, a primer set was used that amplifies an mRNA fragment that spans the site of insertion of the neomycin resistance cassette in the knock-out construct. In *lanes 4 – 6*, a primer set was used that amplifies a fragment downstream from the neomycin resistance cassette insertion site. In *lanes 7–9*, a primer set was used that amplifies a fragment of actin mRNA as a control.

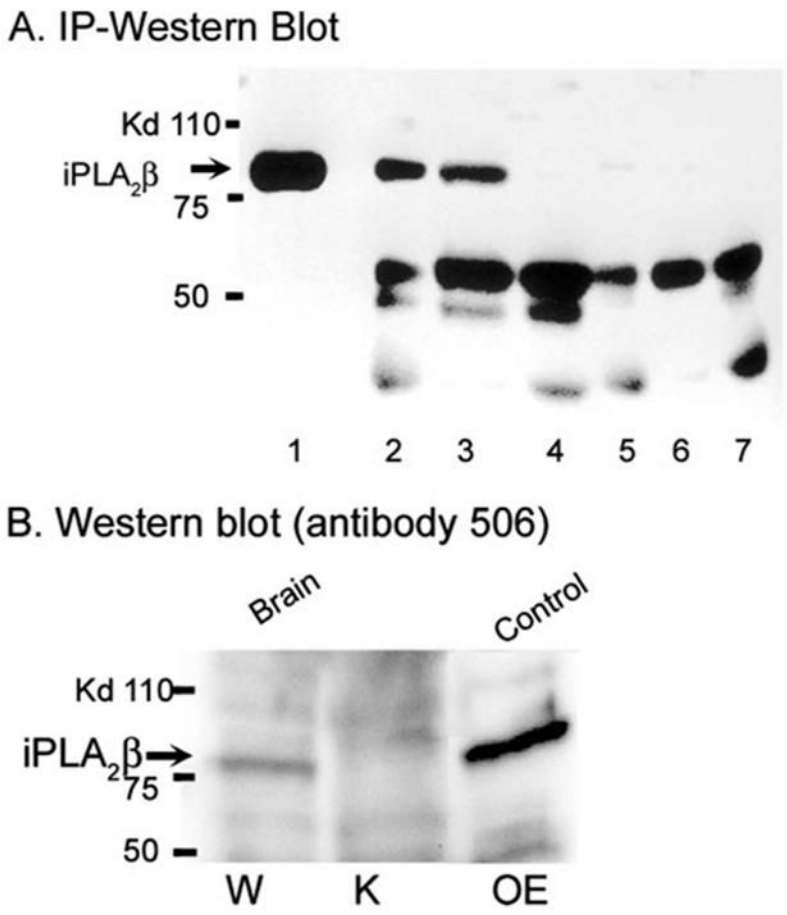

FIGURE 2. Immunoblotting analyses of proteins in tissues of wild-type and iPLA$_2\beta$-null mice that are recognized by iPLA$_2\beta$ antibodies

A represents immunoblots of immunoprecipitates of mouse tissues obtained with an iPLA$_2\beta$ antibody from Cayman Chemical. The immunoprecipitates were analyzed by SDS-PAGE, transferred to nylon membranes, and probed with iPLA$_2\beta$ antibody T14 from Santa Cruz Biotechnology. *Lane 1* represents analysis of an immunoprecipitate from a stably transfected INS-1 insulinoma cell line that overexpresses iPLA$_2\beta$ by more than 10-fold. *Lane 2* represents an immunoprecipitate from a parental INS-1 cell line that expresses lower levels of iPLA$_2\beta$. *Lanes 3* and *4* represent immunoprecipitates from brain of wild-type (*W*) and iPLA$_2\beta$ -knock-out (*K*) mice, respectively. *Lanes 5*, *6*, and *7* represent analyses of washes of immunoprecipitates from INS-1 cells, wild-type brain, and iPLA$_2\beta$-null brain, respectively, and indicate that the iPLA$_2\beta$ anti-body effectively removed the 84-kDa immunoreactive protein, although other cross-reacting proteins of various molecular masses remained. *B* represents immunoblots that were probed with iPLA$_2\beta$ antibody 506 prepared in the laboratory of Dr. Richard Gross. *Lanes 1* and *2* represent analyses of brain cytosol from wild-type and iPLA$_2\beta$-null mice, respectively. *Lane 3* represents an analysis of cytosol from a stably transfected INS-1 cell line that overexpresses iPLA$_2\beta$.

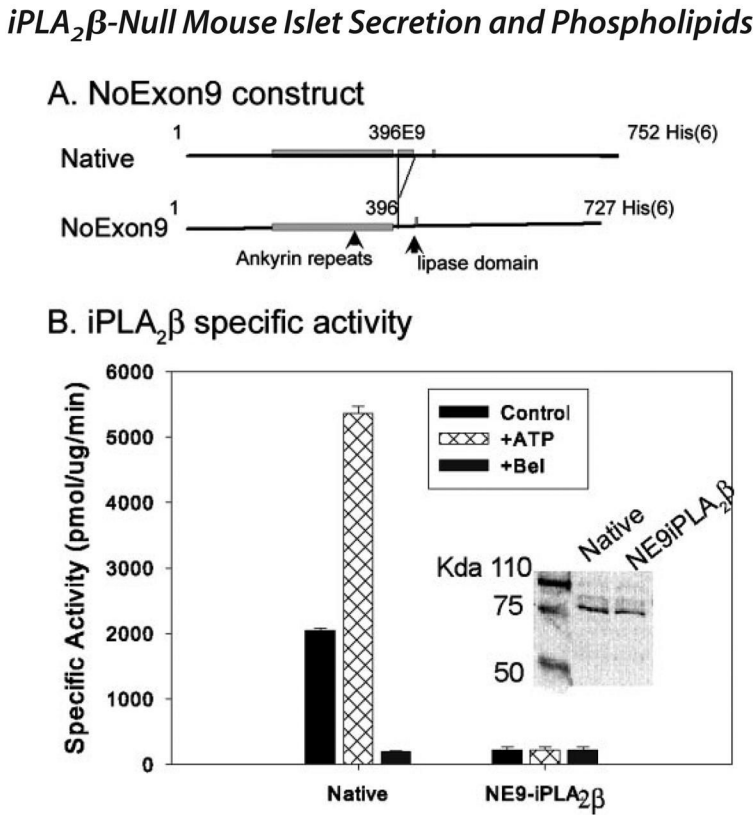

FIGURE 3. Expression of a polyhistidine-tagged iPLA$_2\beta$ mutant protein that lacks sequence encoded by exon 9 of the *iPLA$_2\beta$* gene and determination of its catalytic activity

A illustrates the design of the construct used to prepare the polyhistidine-tagged iPLA$_2\beta$ mutant protein (*NE9iPLA$_2\beta$*) that lacks sequence encoded by exon 9 of the *iPLA$_2\beta$* gene. The positions of the regions of iPLA$_2\beta$ cDNA that encode the ankyrin repeat domain, exon 9, and the GTSTG lipase domain are indicated. The numbers indicate the amino acid residue number in the sequence of the 84-kDa isoform of rat iPLA$_2\beta$. The protein was expressed in a baculovirus-Sf9 cell system, purified by immobilized metal affinity chromatography, and assayed for catalytic activity. *B* represents specific activity measurements for polyhistidine-tagged versions of native iPLA$_2\beta$ (*leftmost set of bars*) and of the NE9-iPLA$_2\beta$ mutant (*rightmost set of bars*). Control (*black bars*) assays were performed in the presence of EGTA and absence of added Ca^{2+}, ATP, or BEL. *Cross-hatched bars* denote assays to which 1 mM ATP was added, and *gray bars* denote assays to which 10 μM BEL was added. Displayed values represent mean ± S.E. (n = 6).

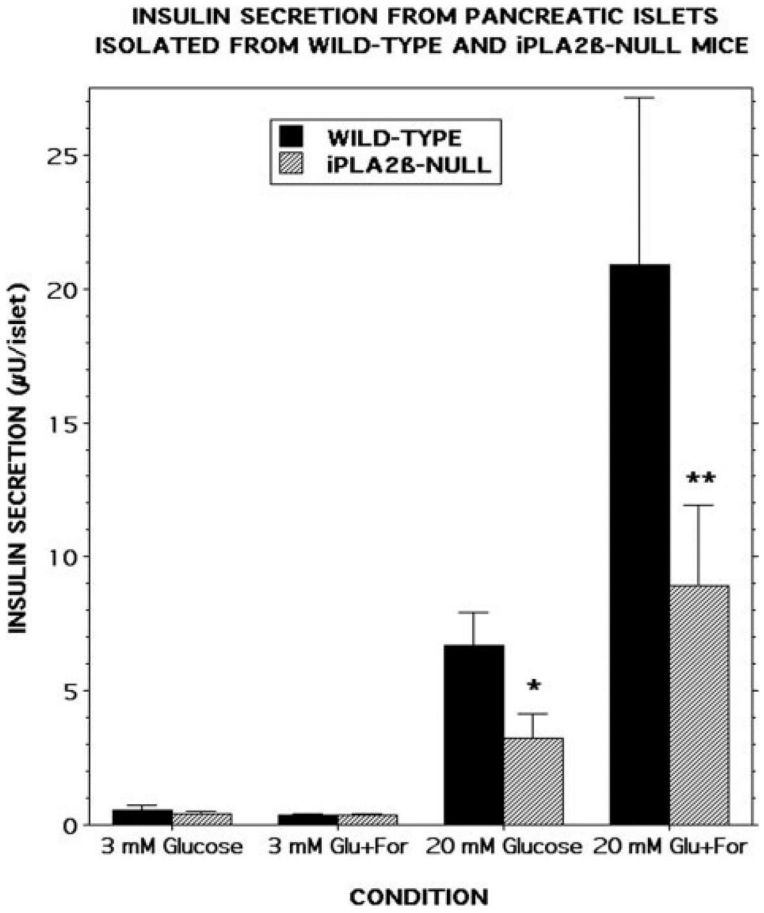

FIGURE 4. Insulin secretion from pancreatic islets isolated from wild-type and iPLA$_2\beta$-null mice

Pancreatic islets were isolated from wild-type (*black bars*) or iPLA$_2\beta$-null (*cross-hatched bars*) mice and incubated (30 islets/condition, 30 min, 37 °C) at a glucose concentration of 3 mM or 20 mM in the absence or presence of 2.5 μM forskolin. Medium was then removed for measurement of insulin by radioimmunoassay. Values represent mean ± S.E. (n = 7). *Single asterisk* denotes $p < 0.01$, and *double asterisk* denotes $p < 0.003$ *versus* wild-type.

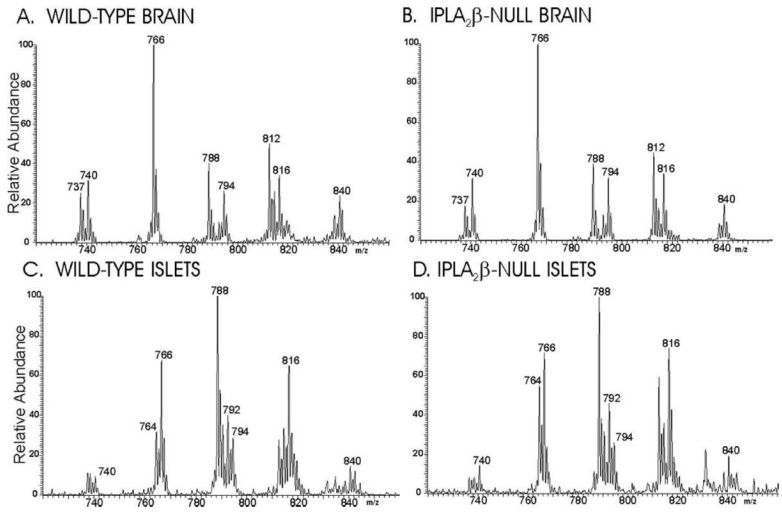

FIGURE 5. Electrospray ionization mass spectrometric analyses of glycerophosphocholine lipids from brain and pancreatic islets of wild-type and iPLA$_2\beta$-null mice

Phospholipids from wild-type (*A* and *C*) or iPLA$_2\beta$-null (*B* and *D*) mouse brain (*A* and *C*), or pancreatic islets (*B* and *D*) were analyzed as Li^+ adducts by positive ion ESI/MS, and the relative abundances of the ion currents were plotted as a function of *m*/*z* value.

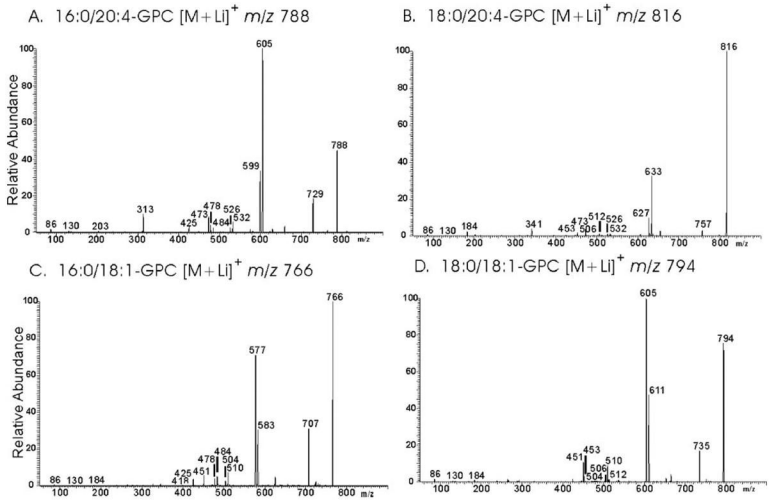

FIGURE 6. Tandem mass spectra of glycerophosphocholine lipids from mouse brain and islets

GPC lipid-Li^+ adducts from wild-type or $iPLA_2\beta$-null mouse brain extracts were analyzed by positive ion ESI/MS/MS. Specific ions were selected in the first mass-analyzing quadrupole and accelerated into the collision cell to induce CAD. Product ions were analyzed in the final quadrupole. Ions selected in the first quadrupole included *m*/*z* 788 (*A*), 816 (*B*), 766 (*C*), and 794 (*D*).

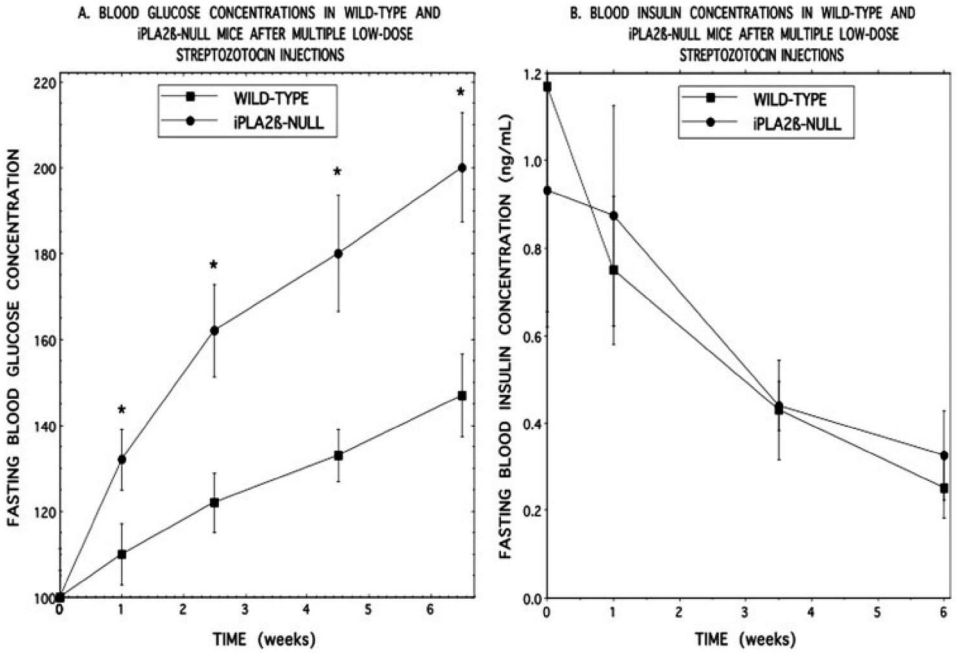

FIGURE 7. Fasting blood glucose and insulin concentrations as a function of time after administration of multiple low doses of streptozotocin to wild-type or iPLA$_2\beta$-null mice

Wild-type (*closed squares*) or iPLA$_2\beta$-null (*closed circles*) mice 12–16 weeks of age were treated with five daily intraperitoneal injections of streptozotocin and then maintained on a normal chow diet. Fasting blood glucose (*A*) and insulin (*B*) concentrations were determined at various intervals after the first streptozotocin injection. Glucose values are expressed as percent of the time 0 value on the day before the first streptozotocin injection and represent mean ± S.E. (n = 14). *Asterisk* denotes $p \leq 0.05$ *versus* wild-type. Insulin concentrations are expressed in ng/ml as mean ± S.E. (n = 14).

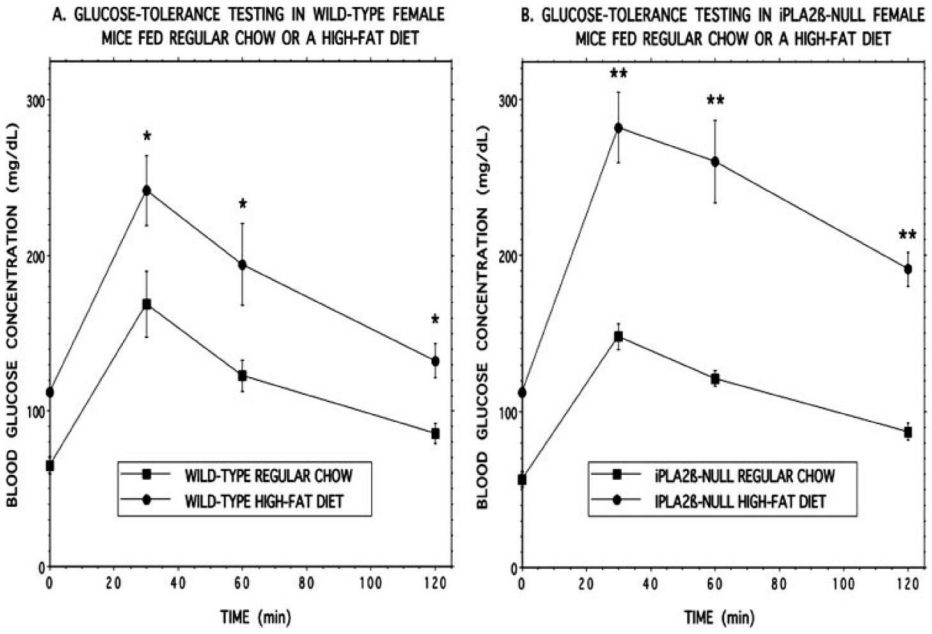

FIGURE 8. Glucose tolerance testing of wild-type and iPLA$_2\beta$-null mice that had been maintained on normal chow or a high fat diet

Wild-type (*A*) or iPLA$_2\beta$-null (*B*) mice were fed a normal mouse chow diet after weaning until they were 8 weeks of age. Thereafter, they were randomized to receive normal chow (*closed squares*) or a high fat diet (*closed circles*) for 6 months. Intraperitoneal glucose-tolerance testing was then performed after an overnight fast. Values represent mean ± S.E. (n = 18). A *single asterisk* denotes $p < 0.05$, and a *double asterisk* denotes $p < 0.005$ *versus* normal chow.

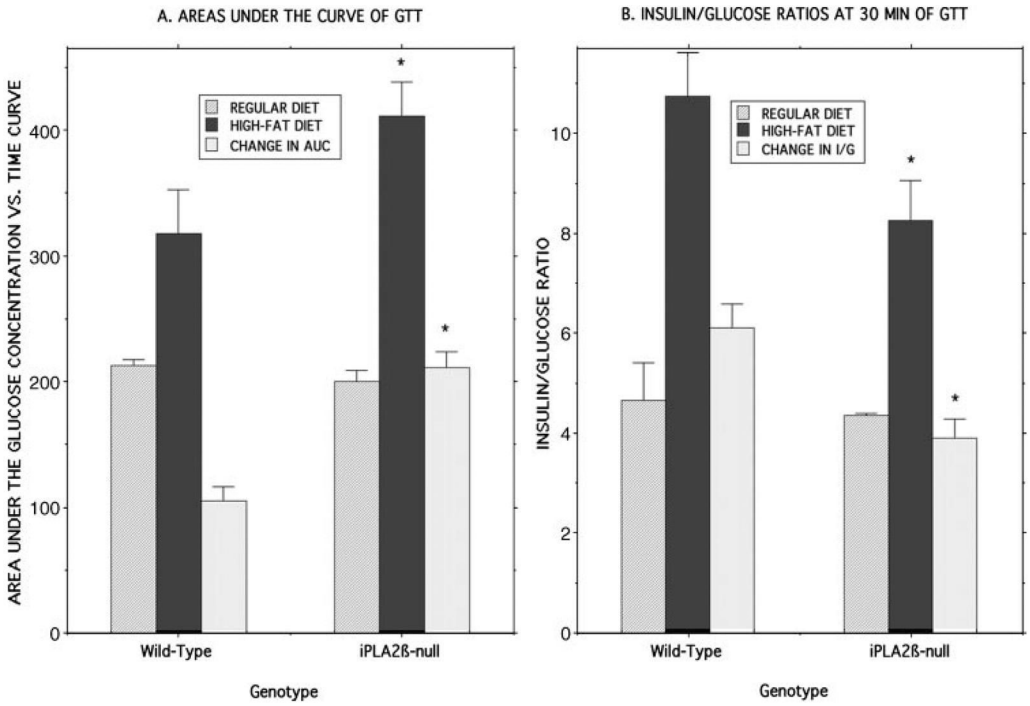

FIGURE 9. Areas under glucose concentration *versus* time curves and blood insulin/glucose ratios in glucose-tolerance testing of wild-type and iPLA$_2\beta$-null mice that had been maintained on normal chow or a high fat diet

Experiments were performed as described in the legends of Fig. 8 and Table 1, and the areas under the glucose concentration *versus* time curves (*A*) and the 30-min blood glucose/insulin concentration ratios (*B*) were determined (107) after intraperitoneal glucose administration for wild-type and iPLA$_2\beta$-null mice that had been fed regular chow (*lightly cross-hatched bars*) or a high fat diet (*dark bars*). Differences between the values obtained with the regular and high fat diets were also computed (*lightly shaded bars*). Displayed values represent mean ± S.E. ($n = 18$), and *asterisks* denote $p < 0.05$ for the comparison between wild-type and iPLA$_2\beta$-null mice.

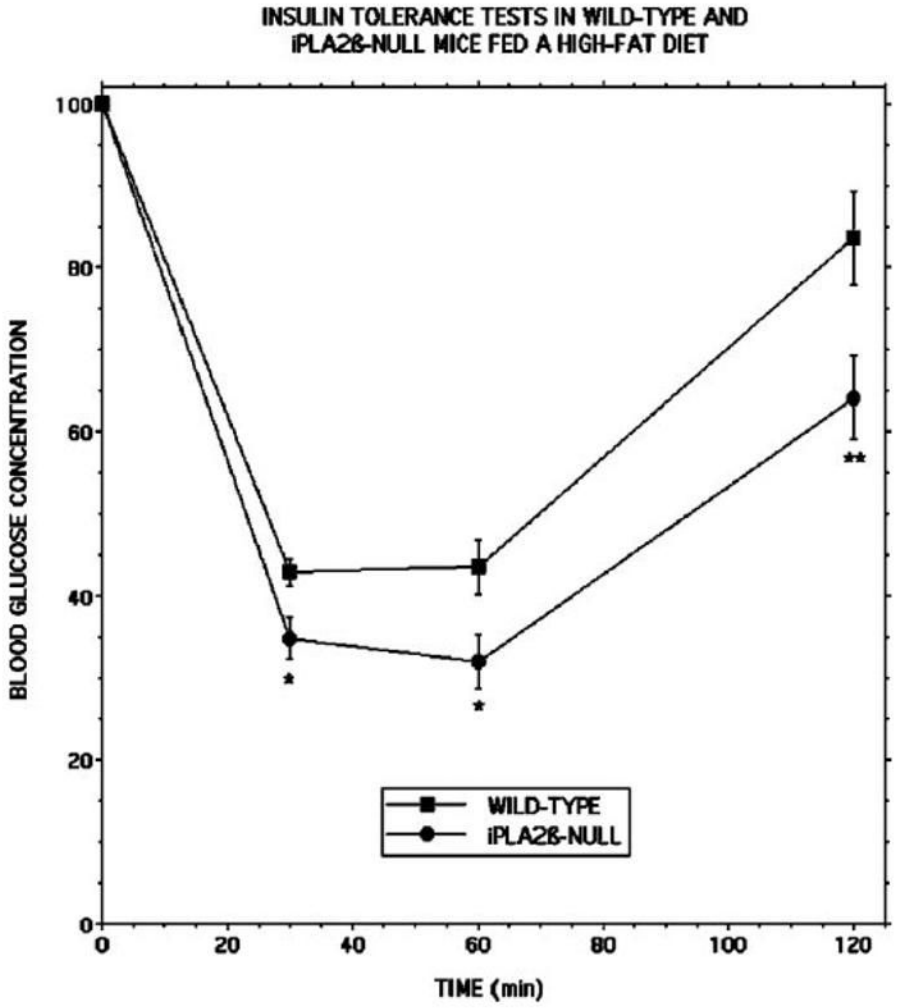

FIGURE 10. Insulin tolerance testing of wild-type and iPLA$_2\beta$-null mice that had been maintained on normal chow or a high fat diet

Wild-type (*closed squares*) or iPLA$_2\beta$-null (*closed circles*) mice were fed a normal mouse chow diet after weaning until they were 8 weeks of age and were then fed a high fat diet for the next 6 months. Intraperitoneal insulin tolerance testing was then performed after an overnight fast. Values represent mean ± S.E. (n = 24). A *single asterisk* denotes $p < 0.02$, and a *double asterisk* denotes $p < 0.002$ *versus* wild-type.

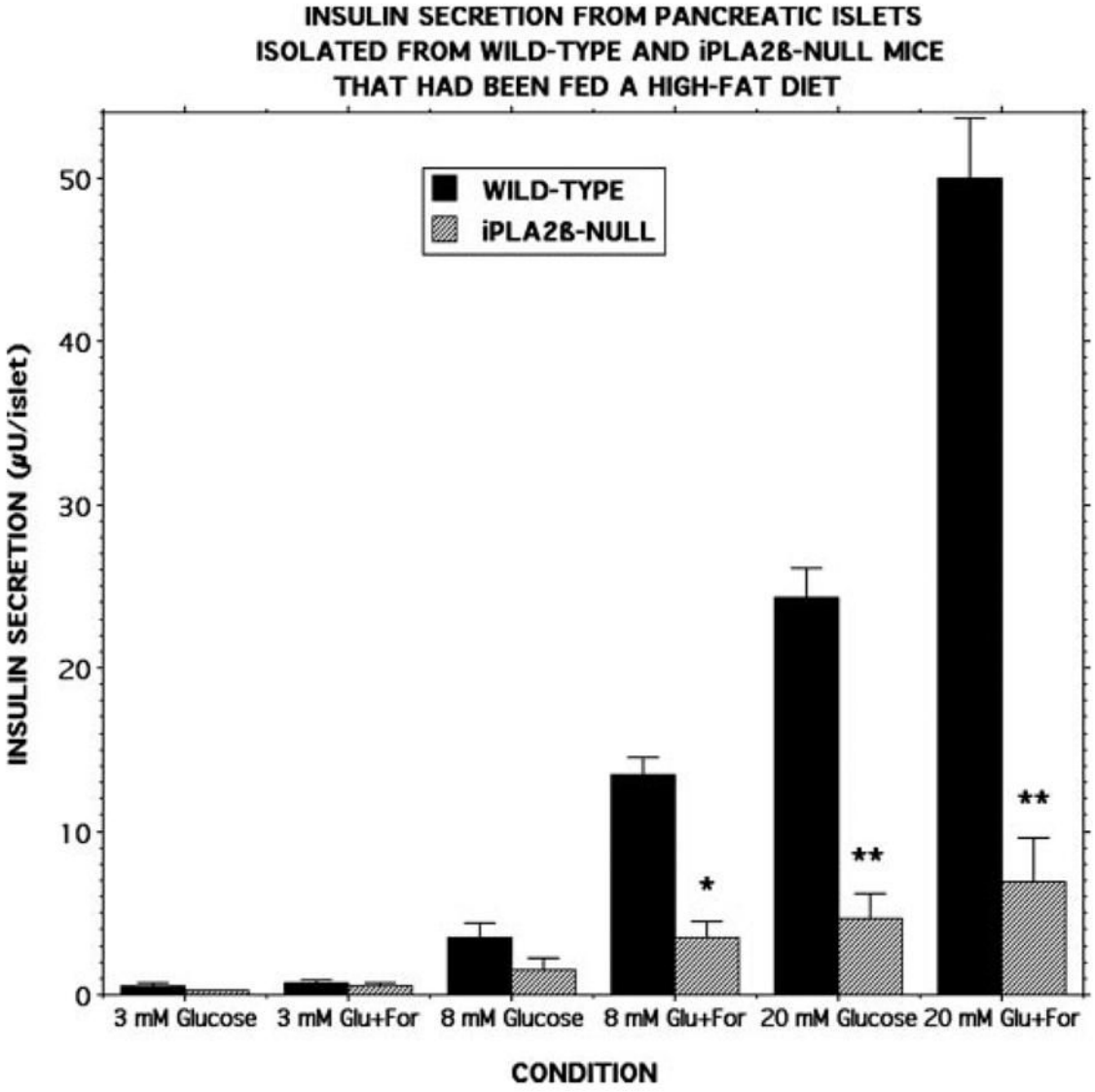

FIGURE 11. Insulin secretion from pancreatic islets isolated from wild-type and iPLA$_2\beta$-null mice that had been fed a high fat diet

Pancreatic islets were isolated from wild-type (*black bars*) or iPLA$_2\beta$-null (*cross-hatched bars*) mice that had been fed a high fat diet and incubated (30 islets/condition, 30 min, 37 °C) at a glucose concentration of 3, 8, or 20 mM in the absence or presence of 2.5 μM forskolin. Medium was then removed for measurement of insulin by radioimmunoassay. Values represent mean ± S.E. (n = 7). *Single asterisk* denotes $p < 0.01$, and *double asterisk* denotes $p < 0.001$ *versus* wild-type.

TABLE 1

Blood insulin levels after intraperitoneal administration of glucose to wild-type and iPLA$_2$β-null mice that had been maintained on normal chow or a high fat diet

Wild-type or iPLA$_2$β-knock-out mice were fed a normal mouse chow diet after weaning until they were 8 weeks of age. Thereafter, they were randomized to receive normal chow regular diet (R) or a high fat diet (HF) for 6 months. An intraperitoneal glucose load was then administered after an overnight fast, and insulin levels were measured in blood samples obtained just before and 30 min after glucose administration. Values represent mean ± S.E. (n = 18).

Genotype	Diet	Time after glucose injection	Insulin
		min	*pg/ml*
WT	R	0	323 ± 048
WT	R	30	781 ± 129
KO	R	0	296 ± 047
KO	R	30	644 ± 006
WT	HF	0	1080 ± 143
WT	HF	30	2600 ± 220
KO	HF	0	990 ± 129
KO	HF	30	2330 ± 227